QUICK LOOK REPORT ON

SEMISCALE MOD-1 TESTS S-28-3 AND S-28-4

STEAM GENERATOR TUBE RUPTURE TESTS

SEMISCALE PROGRAM

July 1977

Prepared for the

U. S. Nuclear Regulatory Commission

EG&G Idaho, Inc.

IDAHO NATIONAL ENGINEERING LABORATORY

ENERGY RESEARCH AND DEVELOPMENT ADMINISTRATION

IDAHO OPERATIONS OFFICE UNDER CONTRACT EY-76-C-07-1570

PRELIMINARY

QUICK LOOK REPORT ON

SEMISCALE MOD-1 TESTS S-28-3 AND S-28-4

STEAM GENERATOR TUBE RUPTURE TESTS

Author: J. M. Cozzuol

Analysts: G. G. Loomis
O. M. Hanner
M. King

SEMISCALE PROGRAM

Approved: D. J. Olson / PDM

D. J. Olson, Manager
Semiscale Program

Approved: DJ Hanson

D. J. Hanson, Manager
Semiscale Experiment Specification & Analysis Branch

The information contained in this summary report is preliminary and incomplete. Selected pertinent data are presented in order to draw preliminary conclusions and to expedite the reporting of research results.

PRELIMINARY

PRELIMINARY

List of Figures

PRELIMINARY

List of Figures (contd)

Summary

This report presents a preliminary evaluation of the results from Semiscale Mod-1 Tests S-28-3 and S-28-4. These integral blowdown-reflood tests were conducted with a break configuration representative of a 200% double-ended offset shear cold leg break, and included the simulation of steam generator tube ruptures at the initiation of vessel refill. Tests S-28-3 and S-28-4 are part of a series of tests (designated the steam generator tube rupture test series) designed to evaluate the effect of a steam generator secondary-to-primary flow on the system and core thermal-hydraulic response during a large break loss-of-coolant experiment. Previous tests in the steam generator tube rupture test series established upper and lower limits on the range of steam generator tube rupture flow rates for which high rod cladding temperatures could occur. The primary purpose of Tests S-28-3 and S-28-4 was to provide experimental results of the effect of steam generator tube rupture flow rates within the range of tube rupture flow rates bounded by the previous tests.

The test conditions for Tests S-28-3 and S-28-4 were essentially the same as those of the Series 28 baseline test (Test S-04-6), except for the introduction of the secondary-to-primary mass flow to simulate the steam generator tube ruptures. The tube rupture flow was simulated by a controlled injection from a heated accumulator tank into the intact loop hot leg between the steam generator inlet plenum and the pressurizer. The steam generator secondary-to-primary flow for Test S-28-3 simulated the flow from the single-ended rupture of a total of 12 tubes in 3 of 4 steam generators in a four-loop PWR. The secondary-to-primary flow for Test S-28-4 simulated the flow from the rupture of a total of 30 tubes in 3 of 4 steam generators in a four-loop PWR. The steam generator tube rupture flow was begun at the initiation of refill (at about 40 seconds after rupture) for both tests. The water in the heated accumulator tank was maintained at about 547°K (approximately the average temperature of the PWR steam generator secondary fluid at rated load) and 7584 kPa. During the period of tube rupture flow, the heat transfer potential of the intact loop steam generator was simulated by discharging (to atmosphere) the steam generator secondary fluid at a rate equivalent to the tube rupture injection rate.

The relatively small steam generator tube rupture flow for Test S-28-3 resulted in a system and core thermal-hydraulic response that was similar to the response observed in Test S-28-2 for which the tube rupture flow rate was about half that for Test S-28-3. The steam generator tube rupture flow in Test S-28-3 caused the core flow to remain negative only until the initiation of the intact loop accumulator nitrogen injection. The initiation of nitrogen injection at about 52 seconds after rupture forced the initiation of vessel refill and resulted in core reflood beginning at about 64 seconds. Reflooding of the core by fluid from the low pressure injection system (LPIS) then continued for the remainder of

the tube rupture flow period. The secondary-to-primary flow during reflood, however, did result in a somewhat lower core reflood rate than was observed in either the Series 28 baseline test (Test S-04-6), or in Test S-28-2.

The core thermal response for Test S-28-3 was influenced considerably by the steam generator tube rupture flow. The reduced core reflood rate caused by the secondary-to-primary flow in Test S-28-3 resulted in a prolonged period of rod heatup which lead to considerably higher peak cladding temperatures (on the average) during reflood in the upper two-thirds of the core than were observed for Test S-04-6. However, the peak cladding temperatures which occurred during reflood for Test S-28-3 were not significantly different than the peak temperatures that were observed during blowdown. The core maximum cladding temperatures during reflood for Test S-28-3 was 1097°K. The primary effect of the steam generator tube rupture flow on the rod quench behavior was to considerably lengthen the time required for quenching to occur, especially in the upper portion of the core. The lengthening of the quench times is attributed to a reduction of the core reflood rate which, in turn, caused a reduction of liquid droplet entrainment in steam flow upward through the core.

During the period of simulated steam generator tube rupture flow for Test S-28-4, the secondary-to-primary flow was the dominant influence on the overall system and core hydraulic response. The steam generator tube rupture flow caused a strong reverse core flow during most of the injection period. This strong reverse core flow physically delayed the initiation of vessel refill until about 150 seconds (as compared to about 40 seconds for the baseline Test S-04-6) and also delayed the refill of the lower plenum until after the steam generator liquid inventory was depleted at about 368 seconds after rupture. The initiation of reflood was then accomplished by the intact loop low pressure injection system (LPIS) and occurred at about 370 seconds.

The core thermal response for Test S-28-4 was characterized by a top-down quench of most of the core following the initiation of the steam generator secondary-to-primary flow. The relatively good cooling and subsequent quenching of the core are attributed to fairly low quality fluid entering the top of the vessel from the steam generator secondary. Once quenching occurred, the rod cladding temperatures remained near the system saturation temperature until the steam generator injection ceased. Following the cessation of the secondary-to-primary injection, a period of core heatup occurred, but the LPIS flow was sufficient to cause requenching by about 450 seconds. The maximum cladding temperatures during this heatup period did not exceed 600°K. As a result of the excellent core cooling following the initiation of the secondary-to-primary injection, the peak cladding temperatures during the period of the injection in general, did not exceed cladding temperatures during the blowdown period.

Introduction

As part of the overall Semiscale blowdown and emergency core cooling project conducted by EG&G Idaho, Inc., the Semiscale Mod-1 experimental program is used to investigate the thermal and hydraulic phenomena accompanying a hypothesized loss-of-coolant accident (LOCA) in a water-cooled nuclear reactor system. The general objective of the Semiscale Program is to obtain representative integral and separate effects thermal-hydraulic response data to provide an experimental basis for analytical model development and verification.

The purpose of Test Series 28 (designated the steam generator tube rupture test series) is to investigate the influence of the rupture of steam generator tubes on the core and system response during a hypothetical large break loss-of-coolant accident (LOCA). Data from Test Series 28 will be used to determine the sensitivity of core peak cladding temperatures to the magnitude of the flow rate from the secondary side of the steam generator to the primary system. The data will also be used to evaluate the capability of current models to predict the thermal-hydraulic phenomena that are expected to occur during the refill and reflood phases of a LOCA with steam generator tube ruptures.

This document contains a preliminary analysis of the results obtained from the third and fourth tests (designated Tests S-28-3 and S-28-4) of the steam generator tube rupture test series conducted in the Semiscale Mod-1 system. Tests S-28-3 and S-28-4 were both conducted with a break configuration representative of a 200% double-ended offset shear cold leg break. The secondary-to-primary flow due to the rupture of steam generator tubes was simulated by injection of fluid at a temperature typical of a PWR steam generator secondary into the intact loop hot leg between the steam generator inlet plenum and the pressurizer. The injection was accomplished using a pressurized water source. For Test S-28-3 fluid was injected at a rate of approximately 0.104 kg/s to simulate flow from the single-ended rupture of 12 tubes[a] in a PWR steam generator, while for Test S-28-4 fluid was injected at a rate of 0.271 kg/s to simulate the flow from 30 tubes in a PWR steam generator. The steam

[a] To provide a basis for comparing the relative magnitudes of the tube rupture mass flow rates in the Semiscale Mod-1 system and a PWR, the magnitudes of the steam generator secondary-to-primary mass flow rates in the Mod-1 system are presented in terms of the flow rates associated with a given number of single-ended tube ruptures in a PWR steam generator. The secondary-to-primary mass flow rates used in the Semiscale Mod-1 system for the tube rupture test series are core area scaled to a PWR.

generator tube rupture flow for both tests was begun at about 40 seconds[a] after the initiation of the cold leg break, and continued for the duration of the test (640 seconds) for Test S-28-3, and until about 367 seconds for Test S-28-4. The change in heat transfer potential of the steam generator was simulated by discharging the steam generator secondary fluid at a rate equivalent to the rate of the tube rupture flow. The system initial conditions and emergency core coolant (ECC) injection parameters for Tests S-28-3 and S-28-4 were essentially the same as for the baseline test for Series 28, Test S-04-6 (Reference 1).

To assist in understanding the data presented in this report, Figure 1 provides an isometric view of the Mod-1 system together with the general location of the instrumentation. The Semiscale Mod-1 system configuration and the instrumentation for Test Series 28 are described in Reference 2.

The powered heater rod configuration for Tests S-28-3 and S-28-4 was identical to that for Test S-04-6. Figure 2 shows the core heater rod arrangement and includes the location of unpowered and high-powered heater rods. Thirty-six of the 40 heater rods were powered in each test. Four rods (rods C3, F3, D5 and F6) were unpowered to make the core bundle more representative of a PWR fuel assembly containing control rod thimbles and instrument tubes. The three center rods (rods D4, E4, and E5) were operated at a 5% higher peak power density than the remaining 33 powered rods to simulate the radial power profile near a control rod thimble in a PWR fuel assembly. Figure 3 shows the Mod-1 heater rod normalized axial power profile. The low power heater rods had a peak power density of about 37.7 kW/m, whereas the three center rods had a peak power density of about 39.7 kW/m. The initial, portion of the core power decay curves for Tests S-28-3 and S-28-4 are shown in Figures 4 and 5 respectively. For comparison purposes, the core power decay curve for Test S-04-6 is included in the figures.

The specified initial conditions and operational variables together with the actual test conditions for Tests S-28-3 and S-28-4 are listed in Tables I and II respectively. Initial prerupture conditions for each test were compared with the specified prerupture conditions and the differences were judged to be minor. These minor differences in conditions prior to rupture for Tests S-28-3 and S-28-4 did not significantly influence the postrupture system behavior.

[a] Forty seconds is approximately the time at which vessel refill would have begun in the Semiscale Mod-1 system if the steam generator tube rupture injection had not occurred. Analysis indicates that a steam generator tube rupture at the initiation of refill would result in a more sever core thermal response than would occur if the steam generator tubes ruptured either during blowdown or later during reflood.

PRELIMINARY

TABLE I

TEST AND PRERUPTURE CONDITIONS FOR TEST S-28-3

Primary System	Specified Condition	Test Condition
Core Power (AMPCOR-T) (VOLTCOR-T) (MW)	1.44	1.43
System pressure (PV+10) (kPa, gage)	15513 ± 172	15554
Loop temperature		
Intact loop cold leg (RBU-14 (°K)	557.8 ± 1	556
Intact loop hot leg (RBU-2) (°K)	594.4 ± 1	593
Broken loop hot leg (TFB-30) (°K)	591.7 ± 3	591
Core flow rate (FTV-COREIN) L/min	As required to obtain core ΔT	548
Pressure suppression system		
Tank water temperature (TF-PSS-33) (°K)	Ambient	292
Tank water pressure (P-PSS) (kPa, gage)	155 ± 7	141
Pressurizer water (DPU-PRESLL) (kg)	9.07	9.1
Steam generator feedwater temperature (TFU-SGFW) (°K)	497 ± 6	490
Steam generator secondary liquid level (DPU-SG-SEC) (cm)	295 ± 5	257

PRELIMINARY

TABLE I (contd)

TEST AND PRERUPTURE CONDITIONS FOR TEST S-28-3

ECC System	Specified Condition	Test Condition
Accumulator CI-T-1		
Injection location	Intact loop cold leg (Spool piece 14)	
Actuation Pressure (kPa, gage)	4137	4247
Liquid volume (L)	80.1	65
Injection rate (FTU-ACC-1) (L/min)	87	95
N_2 flow duration (sec)	24	32
Accumulator CI-T-2		
Location	Broken loop cold leg (Spool piece 42)	
Actuation Pressure (kPa, gage)	4137	4205
Liquid volume (L)	16.4	12
Injection rate (FTB-ACC2) (L/min)	28.65	30
Accumulator CI-T-3 (Steam generator secondary simulator)		
Injection location	Intact loop hot leg (Spool piece 6)	
Temperature (TFU-SGS3-B) (°K)	547	540
Initial pressure (PU-SG3-T) (kPa, gage)	7584	7720
Liquid volume (L)	144.4	144
Injection rate (FTU-SGS-H) (L/min)	8.14 ± 0.7	7.95
Air actuated valve		
Open (seconds after rupture)	40	40
Close (seconds after rupture)	Remains open	Remains open

PRELIMINARY

TABLE I (contd)

TEST AND PRERUPTURE CONDITIONS FOR TEST S-28-3

ECC System	Specified Condition	Test Condition
Steam generator secondary fluid discharge		
Initial liquid level (cm)	295	257
Flow rate (L/min)	8.14 ± 0.7	N/A
Air actuated valve		
Opening time (sec)	40	39
Closing time (sec)	Remains open	Remains open
Intact loop LPIS		
Location	Cold leg (Spool piece 14)	
Actuation Pressure (kPa, gage)	1034	1151
Injection rate (FTU-LPIS) (L/min)	15.1	17.6
Broken loop LPIS		
Location	Cold leg (Spool piece 42)	
Actuation pressure (kPa, gage)	1034	1000
Injection rate (FTB-LPIS) (L/min)	3.6	4.3
Intact loop HPIS		
Location	Cold leg (Spool piece 14)	
Actuation pressure (kPa, gage)	12411	12400
Injection rate (FTU-HPIS) (L/min)	1.17	2.75
Broken loop HPIS		
Location	Cold leg (Spool piece 42)	
Actuation pressure (kPa, gage)	12411	12400
Injection rate (FTB-HPIS) (L/min)	0.68	1.2

PRELIMINARY

TABLE II

TEST AND PRERUPTURE CONDITIONS FOR TEST S-28-4

Primary System	Specified Condition	Test Condition
Core power (AMPCORR-T) (VOLTCOR-T) (MW)	1.44	1.43
System pressure (PV ± 10) (kPa, gage)	15513 ± 172	15513
Loop temperature		
Intact loop cold leg (RBU-14) (°K)	557.8 ± 1	557
Intact loop hot leg (RBU-2) (°K)	594.4 ± 1	594
Broken loop hot leg (TFB-30) (°K)	591.7 ± 3	592
Core flow rate (FTV-COREIN) (L/min)	As required to obtain core ΔT	530
Pressure suppression system		
Tank water temperature (TF-PSS-33) (°K)	Ambient	293
Tank water pressure (P-PSS) (kPa, gage)	155 ± 7	124
Pressurizer water (DPU-PRESLL) (kg)	9.07	8.9
Steam generator feedwater temperature (TRU-SGFW) (°K)	497 ± 6	478
Steam generator secondary liquid level (DPU-SG-SEC) (m)	295 ± 5	257

PRELIMINARY

TABLE II (contd)

TEST AND PRERUPTURE CONDITIONS FOR TEST S-28-4

ECC System	Specified Condition	Test Condition
Accumulator CI-T-1		
Injection location	Intact loop cold leg (Spool piece 14)	
Actuation Pressure (kPa, gage)	4137	4192
Liquid volume (L)	80.1	79
Injection rate (FTU-ACC-1) (L/min)	87	95
N_2 flow duration (sec)	24	25
Accumulator CI-T-2		
Location	Broken loop cold leg (Spool piece 42)	
Actuation Pressure (kPa, gage)	4137	4219
Liquid volume (L)	16.4	12
Injection rate (FTB-ACC2) (L/min)	28.65	28
Accumulator CI-T-3 (Steam generator secondary simulator)		
Injection location	Intact loop hot leg (Spool piece 5)	
Temperature (TFU-SGS3-B) (°K)	547	543
Initial Pressure (PU-SG3-T) (kPa, gage)	7584	7570
Liquid volume (L)	144.4	117
Injection rate (FTU-SGS-H) (L/min)	21.4 $\pm$ 1	21.4
Air acutated valve		
Open (Seconds after rupture)	40	40
Close (Seconds after rupture)	445	368

PRELIMINARY

PRELIMINARY

TABLE II (contd)

TEST AND PRERUPTURE CONDITIONS FOR TEST S-28-4

ECC System	Specified Condition	Test Condition
Steam generator secondary fluid discharge		
Initial liquid level (cm)	295 ± 5	257
Flow rate (L/min)	21.4 ± 1	N/A
Air actuated valve		
Opening time (sec)	40	40
Closing time (sec)	445	N/A
Intact loop LPIS		
Location	Cold leg (Spool piece 14)	
Actuation pressure (kPa, gage)	1034	1090
Injection rate (FTU-LPIS) (L/min)	15.1	17.6
Broken loop LPIS		
Location	Cold leg (Spool piece 42)	
Actuation pressure (kPa, gage)	1034	1078
Injection rate (FTB-LPIS) (L/min)	3.6	4.2
Intact loop HPIS		
Location	Cold leg (Spool piece 14)	
Actuation pressure (kPa, gage)	12411	12400
Injection rate (FTU-HPIS) (L/min)	1.17	1.25
Broken loop HPIS		
Location	Cold leg (Spool piece 42)	
Actuation pressure (kPa, gage)	12411	12400
Injection rate (FTB-HPIS) (L/min)	0.38	1.1

PRELIMINARY

Pretest predictions of the thermal-hydraulic response for Test S-28-3 (Reference 3) and Test S-28-4 (Reference 4) were obtained using Test S-04-6 data and the FLOOD4 computer code. The system response during the first 40 seconds of Tests S-28-3 and S-28-4 was expected to be the same as the system response in Test S-04-6. Therefore, Test S-04-6 data was used to provide the initial conditions for the FLOOD4 calculations starting at 40 seconds after rupture. The FLOOD4 code was then used to provide the predictions through the period of the steam generator tube rupture injection until core quenching occurred. The analysis technique used in the test predictions is described in References 3 and 4. Selected comparisons between test predictions and test data are included in this report.

Test Results

The following discussion presents results of a preliminary evaluation of the effect of simulated steam generator tube ruptures on the system and core response during Tests S-28-3 and S-28-4. In considering the sensitivity of the system and core response to the magnitude of the steam generator secondary-to-primary flow rate, Tests S-28-3 and S-28-4 represent two distinct regimes of thermal-hydraulic behavior. In Test S-28-3, the steam generator secondary-to-primary flow was sufficiently small (0.104 kg/s) so that positive core flow persisted during most of the tube rupture injection period. In Test S-28-4, however, the relatively large steam generator secondary-to-primary flow (0.271 kg/s) resulted in a strong negative core flow during the entire period of tube rupture flow. Thus, to facilitate a complete discussion of the effects of the magnitude of the secondary-to-primary flow on the system and core thermal-hydraulic response, results from Tests S-28-3 and S-28-4 are presented in separate sections. The first section discusses the overall system response and the core response for Test S-28-3, while the second section provides a similar discussion for Test S-28-4. Where applicable, results from Tests S-28-3 and S-28-4 are compared with data from the Series 28 baseline test, Test S-04-6. In addition, to provide an evaluation of the effect on the system and core response of different secondary-to-primary flow rates, results from Tests S-28-3 and S-28-4 are compared with the previous steam generator tube rupture tests, Tests S-28-1 and S-28-2[a] (Reference 5). A final section presents comparisons of data for Tests S-28-3 and S-28-4 with selected results from the pretest calculations.

[a] The secondary-to-primary flow rate of 0.54 kg/s for Test S-28-1 was equivalent to the flow associated with the single-ended rupture of 60 tubes in a PWR steam generator, while the secondary-to-primary flow rate of 0.054 kg/s for Test S-28-2 was equivalent to the flow associated with the single-ended rupture of 6 tubes in a PWR steam generator.

PRELIMINARY

System and Core Response During Test S-28-3

The primary objective of Test S-28-3 was to determine the effect on the system and core thermal-hydraulic response during a large break loss-of-coolant experiment of a simulated steam generator tube rupture flow rate equivalent to the flow associated with the single-ended rupture of 12 tubes in a PWR steam generator. The magnitude of the secondary-to-primary flow rate in Test S-28-3 was in the lower portion of the range of tube rupture flow rates for which high rod cladding temperatures could occur.[b] The steam generator secondary-to-primary flow for Test S-28-3 was initiated at the beginning of vessel refill. An analysis of the data for Test S-28-3 has been performed to evaluate the effect of the steam generator secondary-to-primary flow on the thermal-hydraulic response of the system and core. Results of the analysis are presented in the following two sections. The first section deals with the effect of the secondary-to-primary flow on the overall system and core hydraulic response. Special emphasis is placed on those aspects of the system and core hydraulic response which had a significant influence on the core thermal behavior. The second section is primarily concerned with the core thermal response following the initiation of the steam generator tube rupture flow.

System and Core Hydraulic Response During Test S-28-3. The simulated steam generator tube rupture flow for Test S-28-3 was initiated at about 40 seconds after rupture and continued for the duration of the test. The effects of the tube rupture flow on the overall system and core hydraulic response is illustrated by comparing volumetric flow rates at various points in the system for Test S-28-3 with the corresponding volumetric flow rates for the baseline test, Test S-04-6. Figures 6 and 7 compare the volumetric flow rates in the intact loop hot leg near the

[b] The scaling analysis for Test Series 28 indicated that high rod cladding temperatures could occur in the Semiscale Mod-1 core for secondary-to-primary flow rates of between 0.09 and 0.54 kg/s. This range of tube rupture flow rates in the Semiscale Mod-1 system is equivalent to the flow associated with the single-ended rupture of a total of between 10 and 60 tubes in 3 of 4 steam generators in a 4-loop PWR. (For comparison, note that the 4-loop Trojan PWR has approximately 3300 tubes in each of the 4 steam generators). For secondary-to-primary flow rates in the Semiscale system equivalent to the flow from less than 10 or more than 60 tube ruptures in a PWR steam generator the analysis indicates good core cooling exists during the injection period, thus preventing high cladding temperatures.

PRELIMINARY

vessel and at the entrance to the core, respectively for Tests S-28-3 and S-04-6. As indicated in the figures, for Test S-04-6 a flow reversal occurred at both locations at about 40 seconds after rupture indicating that vessel refill had begun. For Test S-28-3 however, the flow at both locations became substantially more negative at the initiation of the steam generator tube rupture flow. The relatively strong reverse core flow and corresponding upward flow in the downcomer resulting from the steam generator tube rupture flow, in turn, prevented penetration of ECC into the downcomer during the early portion of the secondary-to-primary flow period. The secondary-to-primary flow rate for Test S-28-3, however, was not of sufficient magnitude to maintain the strong reverse core flow once the intact loop accumulator nitrogen flow was initiated at about 52 seconds after rupture.[a] As a result, vessel refill began for Test S-28-3 shortly following the initiation of the accumulator nitrogen flow. Figure 8 compares the downcomer collapsed liquid levels obtained from a downcomer differential pressure measurement for Tests S-28-3 and S-04-6. As indicated in the figure the downcomer collapsed liquid level for Test S-28-3 did not begin to increase until shortly after the initiation of accumulator nitrogen injection (at about 52 seconds), whereas for Test S-04-6, the downcomer was essentially full prior to the initiation of nitrogen flow (at about 68 seconds). The considerable increase in the downcomer collapsed liquid level at abut 55 seconds for Test S-28-3 was due primarily to penetration into the downcomer of ECC fluid stored in the vessel inlet annulus and upper portion of the downcomer during the downcomer countercurrent phase of the test. The relatively slow refill of the downcomer for Test S-28-3 (as well as for Test S-04-6) after about 100 seconds was accomplished by the intact loop LPIS.

Once a liquid level was established in the downcomer for Test S-28-3, the hydraulic head was sufficient to overcome the effect of the steam generator tube rupture flow and a slow reflood of the core occurred. Figure 9 compares the core collapsed liquid levels for Tests S-28-3 and S-04-6 obtained from a lower plenum to upper plenum differential pressure measurement. As indicated in the figure, the rate of core reflood after about 150 seconds was somewhat slower for Test S-28-3 than for Test S-04-6. The somewhat slower reflood rate for Test S-28-3 is attributed to the influence of the steam generator tube rupture flow.

<u>Core Thermal Response During Test S-28-3</u>. The effect of the magnitude of the steam generator tube rupture flow on the core thermal response for Test S-28-3 is illustrated by a comparison of rod cladding temperatures at various elevations in the core with cladding temperatures obtained from the baseline test (Test S-04-6) and from a previous steam generator tube rupture test (Test S-28-2) in which the secondary-to-primary flow was approximately half that for Test S-28-3. Figures 10 through 13 compare typical rod cladding temperatures at the 0.23, 0.36, 0.64 and 0.97 m elevation in the core for the three tests. As indicated in the

[a] A low liquid inventory in the intact loop ECC accumulator (see Table I) caused nitrogen flow to be initiated about 17 seconds earlier than specified for Test S-28-3.

figures, the magnitude of the steam generator tube rupture flow for Test S-28-3 had a considerable effect on the core thermal behavior, especially in the upper portion of the core. For Tests S-04-6 and S-28-2, the core reflood rates after about 100 seconds were not significantly different (see Reference 5). As a result, only minor differences in the peak cladding temperatures and times at which quenching occurred were observed in the lower and central portions of the core. These differences in rod thermal behavior were primarily due to a reduction in the entrainment of fluid upward through the core for Test S-28-2 caused by the steam generator tube rupture flow. In Test S-28-3, however, the somewhat larger secondary-to-primary flow rate resulted in a reduced core reflood rate (see Figure 9) and a prolonged period of rod heatup which lead to considerably higher peak cladding temperatures in the upper portion of the core (Figures 12 and 13). Table III lists the peak cladding temperatures and the times at which the peak cladding temperatures occurred for each thermocouple location for Tests S-28-2, S-28-3, and S-04-6. As indicated in the table, the cladding temperatures in the upper two-thirds of the core for Test S-28-3 are considerably higher (on the average) and occur later during the reflood phase of the test than for either Tests S-28-2 or S-04-6. Note however, that the core maximum cladding temperature for the three tests, although occurring at considerably different times during the tests, were not significantly different. The core maximum cladding temperature which were observed for Tests S-04-6, S-28-2, and S-28-3 were 1075, 1092, and 1098°K respectively.

A comparison of the rod quench times for Tests S-28-2, S-28-3 and S-04-6 further illustrates the effects of the rate of the steam generator tube rupture flow on the core thermal response. Table IV lists the quench times for all thermocouple locations in the core for the three tests. As indicated in the table, the primary effect of an increase in the steam generator tube rupture flow rate on the quench behavior is to considerably lengthen the time required for quenching to occur, especially in the upper portion of the core. The lengthening of the quench times with increased secondary-to-primary flow is attributed to a reduction of liquid droplet entrainment in steam flow upward through the core that occurred as a result of the reduction of the core reflood rate.

System and Core Response During Test S-28-4

The primary objective of Test S-28-4 was to determine the effect on the system and core thermal-hydraulic response during a large break loss-of-coolant experiment of a simulated steam generator tube rupture flow rate equivalent to the flow associated with the single-ended rupture of 30 tubes in a PWR steam generator. The magnitude of the secondary-to-primary flow rate in Test S-28-4 was in the upper portion of a range of tube rupture flow rates for which high rod cladding temperatures could occur. The steam generator secondary-to-primary flow for Test S-28-4 was initiated at the beginning of vessel refill. An analysis of the data from Test S-28-4 has provided additional insight into the phenomena

PRELIMINARY

TABLE III

Peak Core Cladding Temperatures and Times at Which Peak Temperatures Occur For Tests S-28-2, S-28-3, and S-04-6

Thermocouple I.D.	Test S-28-2 °K (sec)	Test S-28-3 °K (sec)	Test S-04-6 °K (sec)
E3-05	736 (69)	707 (60)	710 (44)
C7-07	864 (67)	853 (59)	840 (44)
F2-07	779 (69)	749 (61)	765 (52)
E6-08	818 (69)	813 (62)	808 (53)
A4-09	901 (69)	886 (61)	885 (9)
E4-09	857 (10)	792 (62)	863 (10)
G3-13	874 (113)	865 (124)	890 (64)
D2-14	948 (10)	892 (135)	902 (64)
D4-14	850 (78)	879 (135)	860 (64)
E8-14	922 (8)	942 (117)	935 (64)
F4-14	853 (83)	882 (135)	885 (64)
G5-14	889 (69)	893 (124)	921 (58)
C7-15	928 (69)	961 (134)	943 (64)
C4-20	854 (69)	911 (152)	NA
D7-20	969 (9)	984 (136)	966 (9)
E2-20	947 (9)	NA	891 (58)
E3-20	846 (9)	904 (152)	846 (54)
E5-20	883 (69)	978 (152)	903 (54)
F5-20	846 (9)	921 (138)	888 (54)
D1-21	1062 (8)	1046 (8)	1066 (9)
F2-22	932 (9)	940 (138)	NA
E3-24	906 (113)	1006 (152)	934 (64)
G5-24	925 (78)	1035 (152)	982 (62)
D6-25	943 (123)	1072 (152)	959 (64)
F2-25	894 (132)	992 (169)	936 (64)
E5-25	906 (9)	1025 (167)	959 (64)
C4-26	924 (132)	1035 (162)	NA
D8-26	940 (146)	1069 (243)	NA
F5-26	914 (140)	1048 (167)	NA
E4-27	916 (143)	1038 (173)	934 (71)
C5-28	954 (141)	1079 (167)	948 (71)
E6-28	920 (141)	1056 (167)	940 (64)
A4-29	1029 (9)	1074 (169)	NA
A5-29	1068 (9)	1073 (169)	1075 (9)
B5-29	977 (132)	1092 (167)	NA
B6-29	1092 (9)	1091 (173)	1048 (8)
D3-29	904 (155)	1012 (241)	918 (71)
D4-29	906 (155)	1028 (173)	914 (71)

TABLE III (contd)

Peak Core Cladding Temperatures and Times
at Which Peak Temperatures Occur For
Tests S-28-2, S-28-3, and S-04-6

Thermocouple I.D.	Test S-28-2 °K (sec)	Test S-28-3 °K (sec)	Test S-04-6 °K (sec)
E8-29	968 (132)	1097 (163)	997 (71)
F4-29	913 (153)	1037 (173)	940 (71)
G4-29	925 (151)	1042 (169)	968 (71)
B3-32	879 (162)	1007 (250)	819 (9)
H5-32	933 (151)	1039 (248)	946 (71)
B5-33	950 (155)	1070 (246)	856 (84)
E1-33	898 (151)	1009 (248)	819 (162)
E2-33	905 (162)	1029 (251)	884 (182)
F5-33	888 (172)	1040 (248)	916 (71)
G4-33	900 (157)	1032 (246)	921 (70)
E6-37	794 (145)	1026 (251)	810 (60)
C2-38	766 (146)	927 (281)	691 (72)
G4-38	826 (151)	1002 (254)	853 (64)
A4-39	857 (145)	988 (264)	NA
D3-39	810 (157)	994 (264)	715 (75)
E7-44	824 (180)	1020 (283)	768 (189)
F4-44	808 (198)	988 (292)	703 (84)
A5-45	820 (180)	972 (307)	692 (8)
C4-53	654 (177)	897 (310)	619 (0)
C6-53	706 (168)	926 (310)	638 (0)
F5-53	690 (174)	912 (311)	609 (0)
E4-55	699 (176)	919 (334)	633 (0)
D2-61	631 (198)	783 (338)	608 (0)

PRELIMINARY

TABLE IV

Rod Quench Times for Tests S-28-2, S-28-3, and S-04-6

Thermocouple I.D.	Test S-28-2 (sec)	Test S-28-3 (sec)	Test S-04-6 (sec)
E3-05	92	75	77
C7-07	107	124	86
F2-07	102	115	84
E6-08	106	127	88
A4-09	120	144	95
E4-09	116	138	93
G3-13	145	175	108
D2-14	146	177	109
D4-14	142	174	103
E8-14	149	177	107
F4-14	142	176	106
G5-14	144	175	111
C7-15	161	192	135
C4-20	177	224	NA
D7-20	178	221	191
E2-20	174	NA	184
E3-20	166	222	97
E5-20	175	231	115
F5-20	170	223	112
D1-21	183	251	140
F2-22	185	250	NA
E3-24	186	269	106
G5-24	192	274	208
D6-25	198	295	195
F2-25	207	301	196
E5-25	195	283	184
C4-26	207	314	NA
D8-26	260	407	NA
F5-26	202	315	202
E4-27	217	329	236
C5-28	215	343	220
E6-28	213	330	210
A4-29	229	355	NA
A5-29	228	353	230
B5-29	223	345	NA
B6-29	234	361	188
D3-29	220	348	242
D4-29	220	348	227

PRELIMINARY

PRELIMINARY

TABLE IV

Rod Quench Times for Tests S-28-2, S-28-3, and S-04-6

Thermocouple I.D.	Test S-28-2 (sec)	Test S-28-3 (sec)	Test S-04-6 (sec)
E8-29	223	346	234
F4-29	221	346	238
G4-29	221	345	240
B3-32	260	397	98
H5-32	264	402	294
B5-33	253	394	183
E1-33	263	402	184
E2-33	252	397	248
F5-33	251	400	265
G4-33	251	397	276
E6-37	223	431	107
C2-38	221	435	80
G4-38	246	436	269
A4-39	259	439	NA
D3-39	223	439	85
E7-44	309	479	298
F4-44	305	481	99
A5-45	322	482	99
C4-53	224	489	298
C6-53	240	488	63
F5-53	246	498	68
E4-55	349	505	71
D2-61	368	533	78

PRELIMINARY

which occur in the Semiscale Mod-1 system as a result of the simulated rupture of a comparatively large number of steam generator tubes. The first part of the following discussion is concerned with an evaluation of the overall system hydraulic response both during and following the steam generator tube rupture flow period. The second section deals primarily with the core thermal response following the initiation of steam generator tube rupture flow.

System and Core Hydraulic Response During Test S-28-4 The steam generator tube rupture flow for Test S-28-4 was initiated at about 40 seconds after rupture and continued until about 368 seconds after rupture[a]. During the period of injection, the secondary-to-primary flow was the dominant influence on the overall system and core hydraulic response. A comparison of the volumetric flow rates at various points in the system illustrates the effect of the secondary-to-primary flow. Figures 14 and 15 compare the volumetric flow rates in the intact loop hot leg near the vessel and at the entrance to the core, respectively, for Tests S-28-4 and S-04-6. As indicated in these figures, the reverse flow through the intact loop hot leg and down through the core for Test S-28-4 became substantially more negative at the initiation of the secondary-to-primary flow, while for Test S-04-6 at about the same time (40 seconds) the core flow became positive indicating the initiation of refill.

The strong reverse flow through the core for Test S-28-4 continued until the initiation of nitrogen flow from the intact loop accumulator at about 68 seconds. During the duration of the intact loop accumulator nitrogen flow (until about 88 seconds) the core flow remained negative at a considerably reduced rate. Once the intact loop accumulator nitrogen flow ceased, however, the magnitude of the core flow did not increase to the value attained prior to the nitrogen injection even though the secondary-to-primary flow continued at essentially the same rate. The considerably smaller reverse core flow after the period of nitrogen injection can be attributed to a change in the resistance to steam flow in the intact loop cold leg. During the period of accumulator liquid

[a] Because of a leak in the steam generator secondary simulator accumulator prior to rupture, the liquid inventory available for injection into the system was considerably lower than specified. As a result, the liquid supply was depleted by about 368 seconds (rather than the specified 445 seconds) which allowed the injection of the pressurizing gas (nitrogen) into the primary system. However, based on an analysis of the system and core hydraulic response (as well as the core thermal response) it is felt that the short duration secondary-to-primary flow and nitrogen injection into the primary system did not significantly affect test results other than to cause a shift in the times at which quenching of the core occurred.

injection into the intact loop cold leg, steam flow from the hot leg to the vessel inlet side of the break was effectively blocked. The effect of the accumulator nitrogen flow, however, was to clear liquid from the intact loop cold leg. This phenomenon is illustrated in Figure 16 which shows the fluid density in the intact loop cold leg. Once the nitrogen flow ceased, an additional path for removal of steam from the intact loop occurred. As a result, the magnitude of the core inlet volumetric flow did not increase significantly, but remained substantially negative until the steam generator secondary-to-primary flow ceased at about 368 seconds. The volumetric flow near the vessel on the vessel inlet side of the broken loop, shown in Figure 17, indicates the substantial increase in the flow rate for Test S-28-4 once the nitrogen flow ceased.

Figure 18 compares the downcomer collapsed liquid level obtained from a downcomer differential pressure measurement for Tests S-28-4 and S-04-6. The figure indicates the relative rate of refill of the downcomer for the two tests. As shown in the figure, refill of the downcomer did not begin until about 150 seconds for Test S-28-4 (approximately the same time that the reverse core flow began to decrease). Partial refill of the downcomer and lower plenum after 150 seconds was accomplished by the intact loop low pressure injection system (LPIS). However, because of the strong reverse core flow, the lower plenum did not completely refill until after the steam generator secondary-to-primary flow stopped at about 368 seconds. Figure 19 compares the collapsed liquid levels obtained from a lower plenum-to-upper plenum differential pressure measurement for Tests S-28-4 and S-04-6. As indicated in the figure only a partial refill of the lower plenum occurred for Test S-28-4 until about 368 seconds, whereas for Test S-04-6 core reflood was occurring during the entire period. The increase in core collapsed liquid level at about 370 seconds for Test S-28-4 is a result of the cessation of the secondary-to-primary flow and corresponds to a reduction in the downcomer collapsed liquid level (Figure 18). Reflood of the core was initiated at about 370 seconds as indicated in Figure 20 which shows the core inlet fluid density for Test S-28-4.

<u>Core Thermal Response During Test S-28-4</u> The core thermal response for Test S-28-4 was characterized by a top down quench of the entire core caused by the steam generator tube rupture flow. Figures 21, 22, and 23 show the rod cladding temperatures at several elevations in the core for rods E4, E6 and F4, respectively. As indicated in the figures, a period of good cooling in the core existed between the initiation of the steam generator tube rupture flow (at about 40 seconds) and the initiation of the intact loop accumulator nitrogen flow (at about 68 seconds). The effect of the accumulator nitrogen flow, however, was to significantly reduce the flow downward through the core (Figure 15) thus causing the short period of heatup indicated in the figures. After the nitrogen flow ceased, the downward flow through the core of the secondary liquid-vapor mixture was sufficient to provide good core cooling and resulted in a top-down quench of most of the core prior to the initiation of core reflood.

PRELIMINARY

Once quenching occurred in Test S-28-4, the cladding temperatures remained near the fluid saturation temperature, until cessation of the secondary-to-primary injection. The cessation of the steam generator tube rupture flow resulted in a reduction of the core flow to zero, which in turn caused dryout of the core heater rods and a resulting gradual increase in the rod cladding temperatures. However, the reflood of the core by LPIS flow (which began at about 370 seconds) was sufficient to requench the core by about 450 seconds (Figures 21 through 23). The maximum cladding temperatures resulting from the dryout did not exceed 600 °K.

The effect of the magnitude of the steam generator tube rupture flow on the core thermal response for Test S-28-4 is illustrated by comparing the peak cladding temperatures at each thermocouple location in the core with the peak cladding temperatures obtained from the baseline test (Test S-04-6) and from a previous steam generator tube rupture test (Tests S-28-1) in which the secondary-to-primary flow was about twice that for Test S-28-4. Table V lists the peak cladding temperatures and the times after rupture at which the peak cladding temperatures occur for each thermocouple location in the core for Tests S-28-1, S-28-4 and S-04-6. As indicated in the table, the peak cladding temperatures at a majority of the thermocouple locations for Test S-28-4 (as well as for Test S-28-1) occurred during the blowdown phase of the test rather than during the steam generator tube rupture injection period[a]. The significantly lower temperatures following the initiation of the tube rupture flow can be attributed to the enhanced core cooling for both tests caused by the fairly low quality liquid-vapor mixture in the core. The considerably smaller secondary-to-primary flow rate for Test S-28-4 (as compared to Test S-28-1) however, resulted in somewhat poorer cooling in the lower part of the core (0-0.38 m elevation) thus causing the delay in peak cladding temperatures indicated in Table V.

A comparison of the rod quench times for Tests S-28-1, S-28-4, and S-04-6 further illustrates the effects of the rate of the steam generator secondary-to-primary flow on the core thermal response. Table VI lists the quench times for all thermocouple locations in the core for the three tests. As illustrated in the table, Test S-28-4 exhibited a top-down quench but at a considerably slower rate than occurred for Test S-28-1. Essentially the entire core had quenched for Test S-28-4 prior to the initiation of core reflood at about 370 seconds. The top-down quench behavior for both Tests S-28-1 and S-28-4 is considerably different than the bottom-top-middle quench behavior observed for Test S-04-6 which was caused by a bottom reflood of the core.

The considerably smaller secondary-to-primary flow rate for Test S-28-4 (as compared to Test S-28-1) resulted in a preferential flow path through the core on the side adjacent to the intact loop hot leg. As indicated

[a] Note that the peak cladding temperatures during blowdown for Test S-28-1 are considerably higher than for either Tests S-28-4 or S-04-6. This difference is attributed to a delay in the initiation of the core power decay of about 1 second for Test S-28-1.

PRELIMINARY

PRELIMINARY

TABLE VI

Core Quench Times for Tests S-28-1, S-28-4, and S-04-6

Thermocouple I. D.	Test S-28-1 (sec)	Test S-28-4 (sec)	Test S-04-6 (sec)
E3-05	94	275	77
C7-07	124	388	86
F2-07	147	390	84
E6-08	111	389	88
A4-09	99	153	95
E4-09	91	197	93
G3-13	115	407	108
D2-14	106	240	109
D4-14	78	148	103
E8-14	184	411	107
F4-14	75	220	106
G5-14	100	267	111
C7-15	110	281	135
C4-20	78	124	NA
D7-20	122	348	191
E2-20	121	NA	184
E3-20	77	194	97
E5-20	77	180	115
F5-20	78	221	112
D1-21	112	227	140
F2-22	145	434	106
E3-24	43	181	106
G5-24	81	208	208
D6-25	83	181	195
F2-25	122	444	196
E5-25	71	170	184
C4-26	67	107	208
D8-26	73	182	217
F5-26	66	181	202
E4-27	67	147	236
C5-28	59	110	220
E6-28	78	197	201
A4-29	69	97	229
A5-29	71	110	230
B5-29	59	102	236
B6-29	74	118	188
D3-29	63	128	242
D4-29	64	114	227
E8-29	131	455	234

PRELIMINARY

TABLE VI (Contd)

Thermocouple I. D.	Test S-28-1 (sec)	Test S-28-4 (sec)	Test S-04-6 (sec)
F4-29	58	162	238
G4-29	66	175	240
B3-32	63	96	98
H5-32	72	164	294
B5-33	51	90	183
E1-33	94	179	184
E2-33	82	464	248
F5-33	56	160	265
G4-33	60	160	277
E6-37	63	159	107
C2-28	56	106	80
G4-38	57	145	269
A4-39	50	81	NA
D3-39	53	106	85
E7-44	73	320	298
F4-44	50	118	99
A5-45	47	74	99
C4-53	45	71	298
C6-53	50	85	63
F5-53	50	115	68
E4-55	46	87	71
D2-61	63	115	78

in Table VI, the rods opposite the intact loop hot leg (eg. rods G3, E8, F2, E2, etc.) exhibit considerably later quench times. This can apparently be attributed to the fact that the rods in the Semiscale Mod-1 system extend through the upper plenum. Apparently the rods on the intact loop hot leg side of the vessel essentially block the liquid portion of the tube rupture flow from penetrating to the opposite side of the vessel. As a result, the cooling of the rods on the side of the vessel opposite the intact loop hot leg is not as good as on the side of the vessel adjacent to the intact loop hot leg.

Comparison of Selected Data to Calculations

Test predictions of the thermal-hydraulic response characteristics for Tests S-28-3 and S-28-4 were performed using the FLOOD4 computer code Detailed descriptions of the analysis technique used in the calculations and additional predicted results for the two tests are given in References 3 and 4.

The predicted and measured cladding temperatures for Test S-28-3 exhibited reasonably good agreement. The FLOOD4 calculation predicted the rod cladding temperature in the middle of the rod high power step would increase 255°K following the initiation of core reflood. This compares to an increase in the measured rod cladding temperature near the middle of the high power step of between about 240 and 160 °K.

A comparison of the predicted an measured rod cladding temperatures for Test S-28-4 indicates that the FLOOD4 calculation considerably overpredicted the measured cladding temperatures during the reflood phase of the test. The peak calculated cladding temperature on the rod high power zone during reflood was about 1175 °K, whereas the peak measured cladding temperature on the high power zone did not exceed 600 °K during the reflood phase of the test. The substantial overprediction of the measured cladding temperatures can be attributed to the method of analysis used in the calculations. In the calculations for Test S-28-4 the transient was divided into four main time periods. These periods consisted of: (1) the blowdown period prior to the steam generator tube rupture, (2) a period of reverse core flow after the tube rupture and lasting until the steam generator secondary empties, (3) heatup of the core as the lower plenum is refilled by the HPIS and LPIS, and (4) core reflood by the LPIS and HPIS. For the second period described above a FLOOD4 calculation was performed to determine the core cooldown rate due to the steam generator tube rupture flow. However, to be conservative, the calculation purposely did not take into account the liquid portion of the flow through the core, and thus did not predict the quenching and corresponding low cladding temperatures obtained during Test S-28-4 (see Figures 21 through 23). As a result, the initial cladding temperatures calculated for the period of heatup and the corresponding initial temperatures calculated for the reflood period were considerably higher than the measured data.

PRELIMINARY

TABLE V

Maximum Core Cladding Temperatures and Times at Which Maximum Temperatures Occur for Tests S-28-1, S-28-4, and S-04-6

Thermocouple I. D.	Test S-28-1 °K (sec)	Test S-28-4 °K (sec)	Test S-04-6 °K (sec)
E3-05	730 (39)	743 (124)	710 (44)
C7-07	864 (39)	858 (94)	840 (44)
F2-07	767 (39)	793 (125)	765 (52)
E6-08	822 (10)	837 (109)	808 (53)
A4-09	928 (10)	882 (9)	885 (9)
E4-09	807 (39)	801 (107)	863 (10)
G3-13	904 (10)	850 (109)	890 (64)
D2-14	965 (10)	838 (105)	902 (64)
D4-14	899 (10)	817 (10)	860 (64)
E8-14	975 (9)	916 (109)	935 (64)
F4-14	881 (10)	844 (109)	885 (64)
G5-14	908 (10)	880 (109)	921 (58)
C7-15	955 (10)	902 (39)	943 (64)
C4-20	913 (10)	831 (9)	NA
D7-20	1010 (10)	896 (39)	966 (9)
E2-20	924 (10)	NA	891 (58)
E3-20	910 (10)	834 (9)	846 (54)
E5-20	951 (10)	868 (39)	903 (54)
F5-20	906 (10)	834 (109)	888 (54)
D1-21	1125 (10)	1050 (8)	1066 (9)
F2-22	1003 (10)	908 (8)	NA
E3-24	1033 (45)	875 (9)	934 (64)
G5-24	970 (10)	913 (109)	982 (62)
D6-25	971 (10)	899 (39)	959 (64)
F2-25	969 (10)	875 (9)	936 (64)
E5-25	968 (10)	880 (10)	959 (64)
C4-26	980 (10)	879 (10)	NA
D8-26	872 (9)	843 (40)	NA
F5-26	963 (10)	884 (10)	NA
E4-27	938 (10)	841 (9)	934 (71)
C5-28	943 (10)	951 (10)	948 (71)
E6-28	945 (10)	887 (109)	940 (64)
A4-29	1058 (10)	933 (10)	NA
A5-29	1123 (9)	914 (8)	1075 (9)
B5-29	971 (10)	890 (40)	NA
B6-29	1064 (9)	980 (8)	1048 (8)
D3-29	964 (10)	863 (9)	918 (71)
D4-29	939 (10)	840 (10)	914 (71)

PRELIMINARY

TABLE V (Contd)

Thermocouple I. D.	Test S-28-1 °K (sec)	Test S-28-4 °K (sec)	Test S-04-6 °K (sec)
E8-29	999 (10)	930 (39)	997 (71)
F4-29	940 (10)	868 (9)	940 (71)
G4-29	953 (10)	869 (9)	968 (71)
B3-32	875 (10)	700 (10)	819 (9)
H5-32	906 (9)	818 (110)	946 (71)
B5-33	871 (10)	828 (10)	856 (84)
E1-33	907 (10)	821 (8)	819 (162)
E2-33	926 (10)	838 (8)	884 (182)
F5-33	863 (9)	819 (9)	916 (71)
G4-33	894 (10)	821 (9)	921 (70)
E6-37	780 (10)	769 (109)	810 (60)
C2-38	779 (11)	686 (100)	691 (72)
G4-38	748 (10)	735 (130)	853 (64)
A4-39	808 (10)	711 (10)	NA
D3-39	791 (10)	688 (99)	715 (75)
E7-44	656 (0)	722 (129)	768 (189)
F4-44	675 (10)	670 (109)	703 (84)
A5-45	677 (13)	669 (0)	692 (8)
C4-53	618 (0)	618 (0)	619 (0)
C6-53	638 (0)	638 (0)	638 (0)
F5-53	613 (0)	612 (0)	609 (0)
E4-55	631 (0)	631 (0)	633 (0)
D2-61	608 (0)	608 (0)	608 (0)

References

(1) H. S. Crapo, B. L. Collins, and K. E. Sackett, "Experiment Data Report for Semiscale Mod-1 Tests S-04-5 and S-04-6 (Baseline ECC Tests)", TREE-NUREG-1045, January 1977.

(2) D. J. Olson Ltr to P. E. Litteneker, DJO-125-77, "Transmittal of Semiscale EOS Appendix 28", June 1977.

(3) D. J. Olson Ltr to R. E. Tiller, DJO-146-77, "Test Prediction of Semiscale Mod-1 Integral Test S-28-3", June 28, 1977.

(4) D. J. Olson Ltr to R. E. Tiller, DJO-144-77, "Test Prediction of Semiscale Mod-1 Integral Test S-28-4", June 30, 1977.

(5) D. J. Olson Ltr to R. E. Tiller, DJO-151-77, "Transmittal of Quick Look Report for Semiscale Mod-1 Steam Generator Tube Rupture Tests S-28-1 and S-28-2", July 6, 1977.

PRELIMINARY

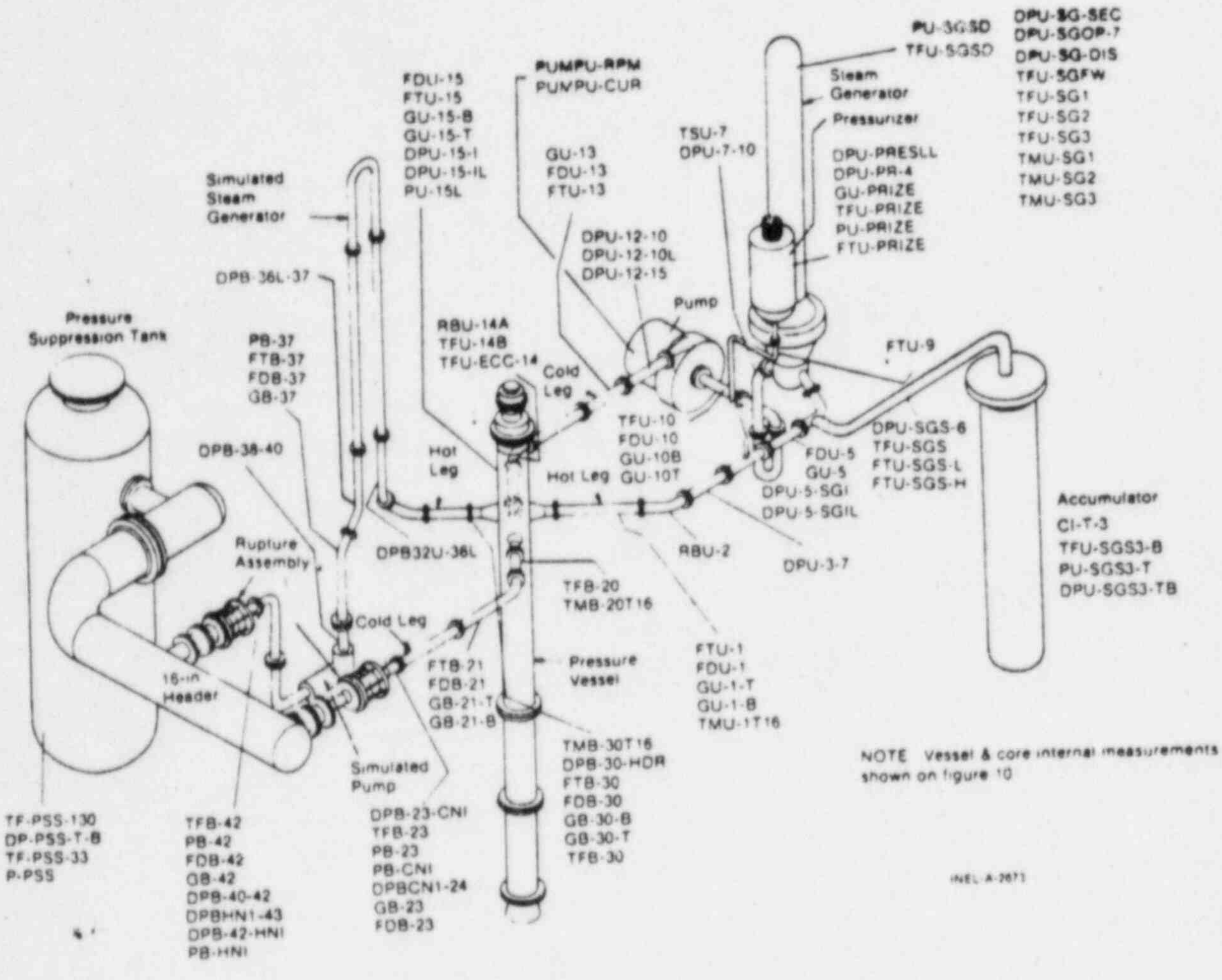

Figure 1. Semiscale Mod-1 System and Instrumentation for Cold Leg Break Configuration - Isometric

PRELIMINARY

PRELIMINARY

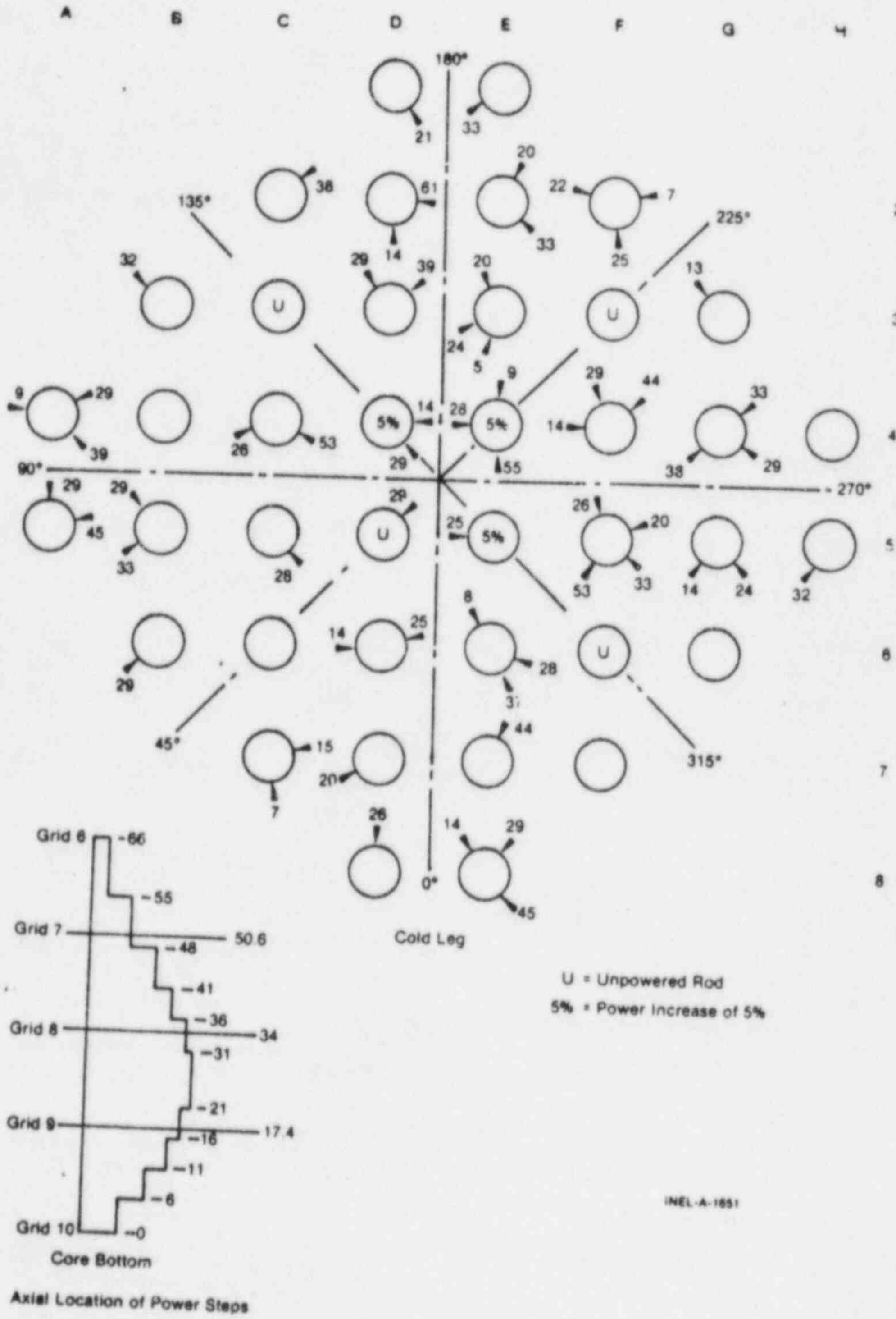

Figure 2. Semiscale Mod-1 Core - Plan View with Thermocouple Locations

PRELIMINARY

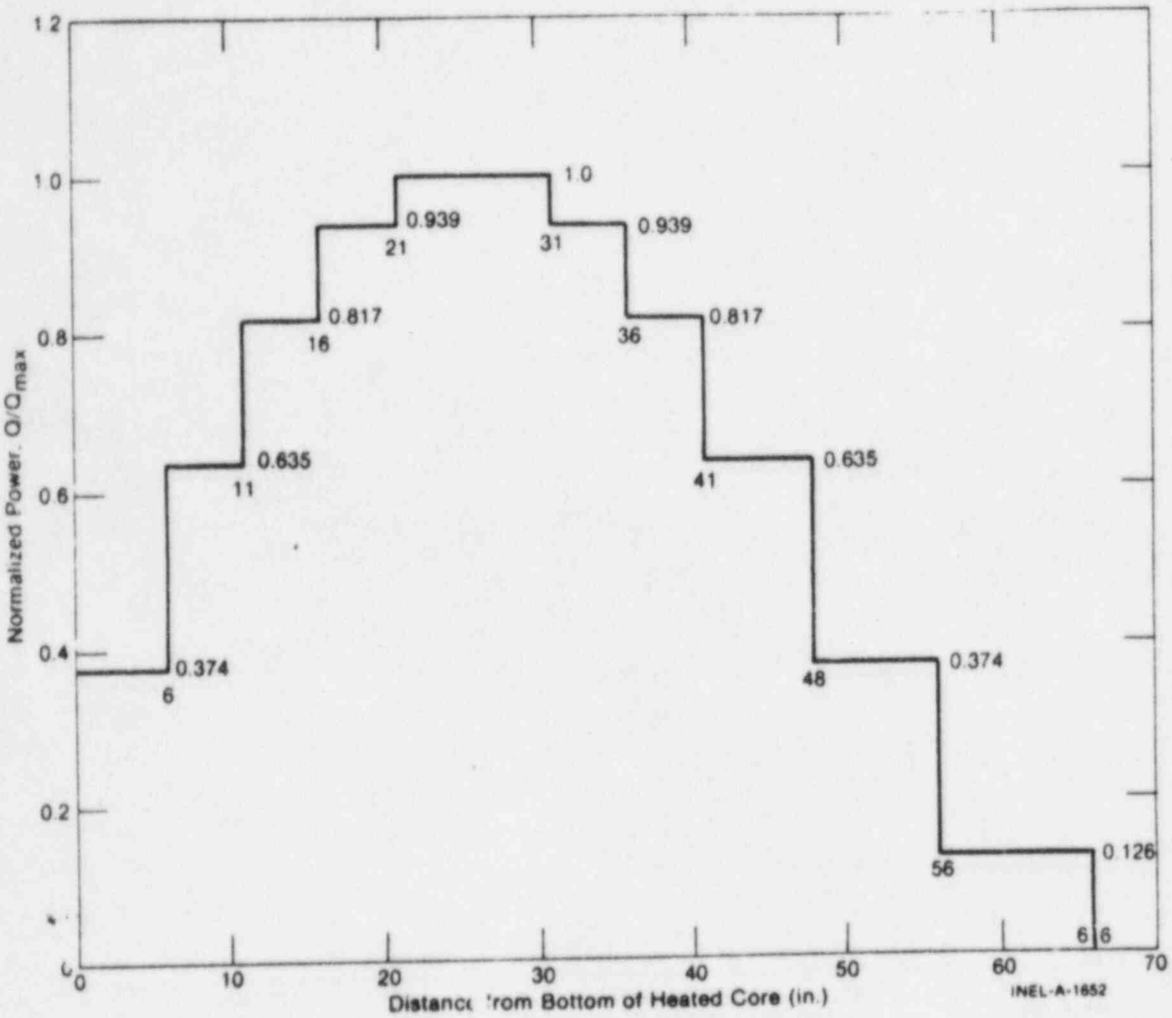

Figure 3. Semiscale Mod-1 Axial Power Profile

PRELIMINARY

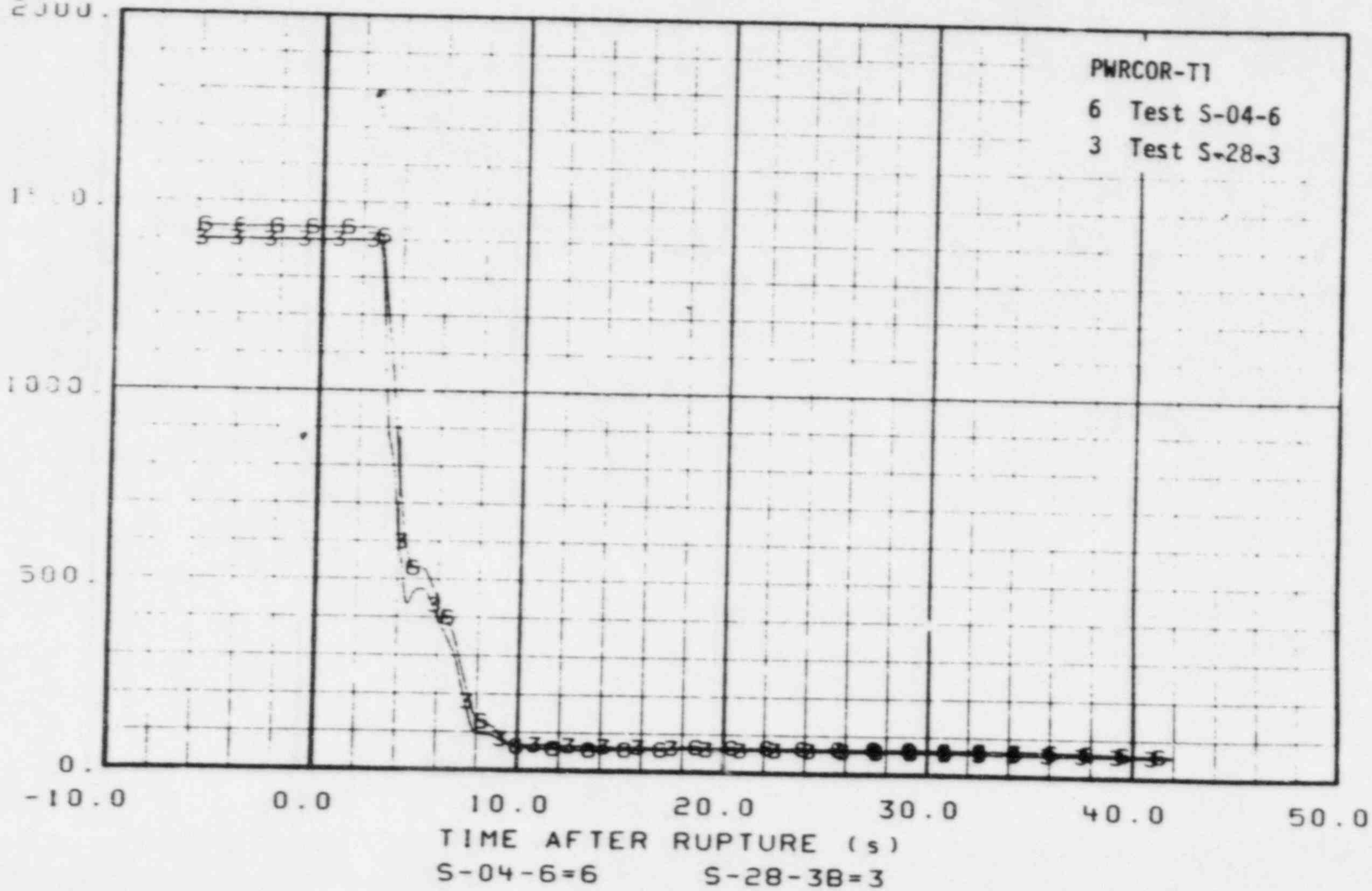

Figure 4. Initial Core Power Decay - Tests S-28-3 and S-04-6

PRELIMINARY

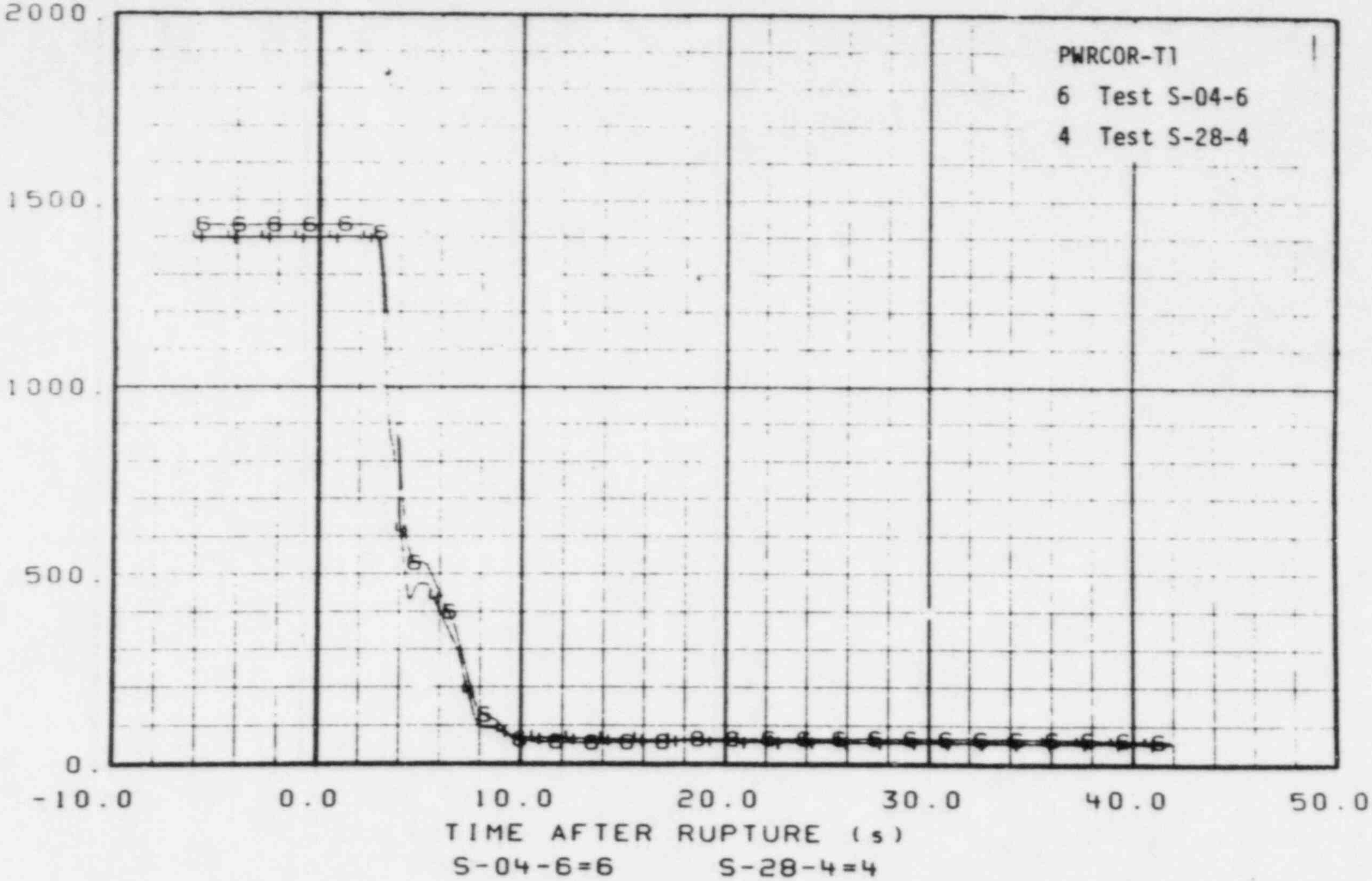

Figure 5. Initial Core Power Decay - Tests S-28-4 and S-04-6

PRELIMINARY

PRELIMINARY

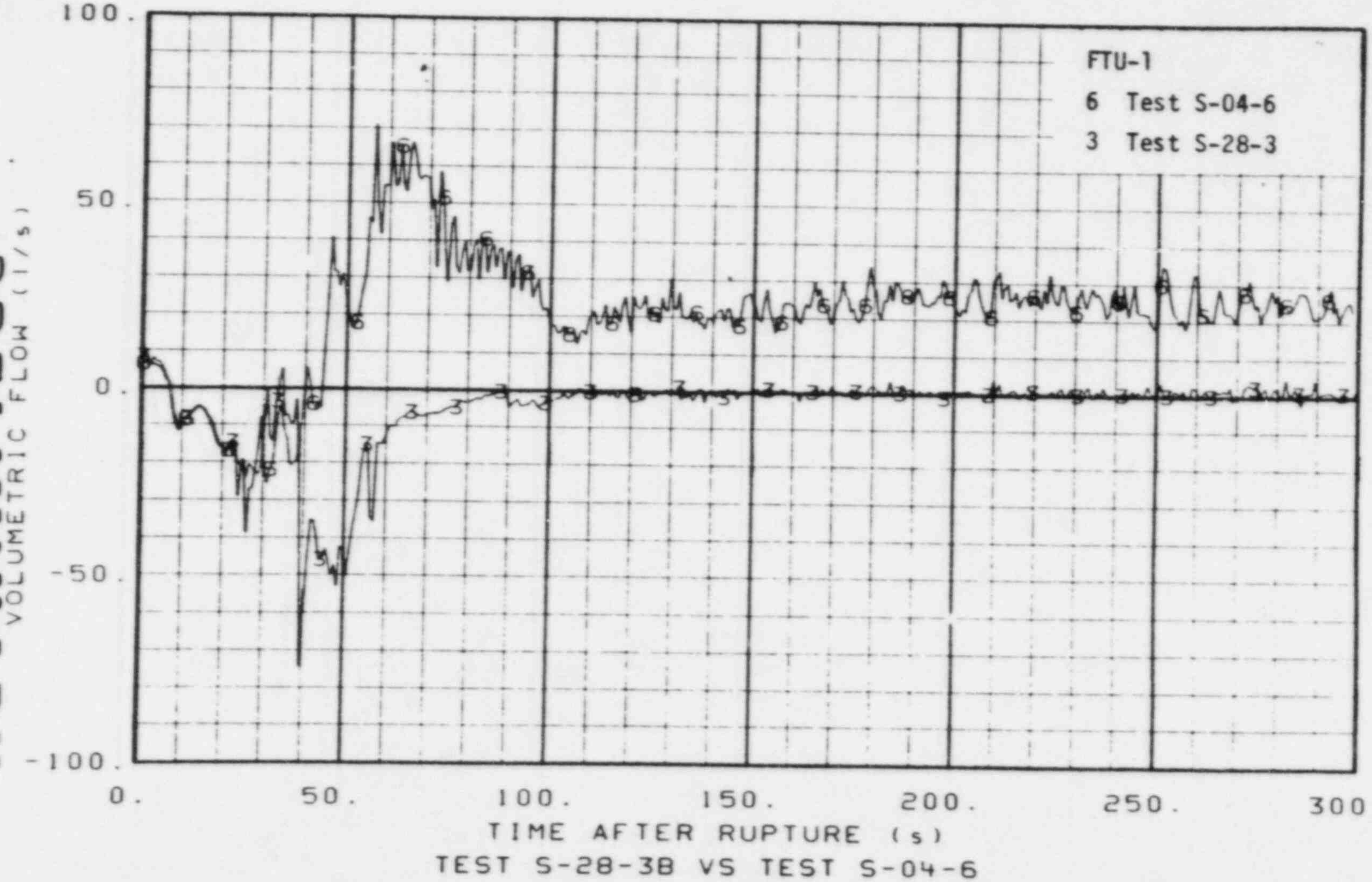

PRELIMINARY

Figure 6. Comparison of Intact Loop Hot Leg Volumetric Flow Near the Vessel - Tests S-28-3 and S-04-6

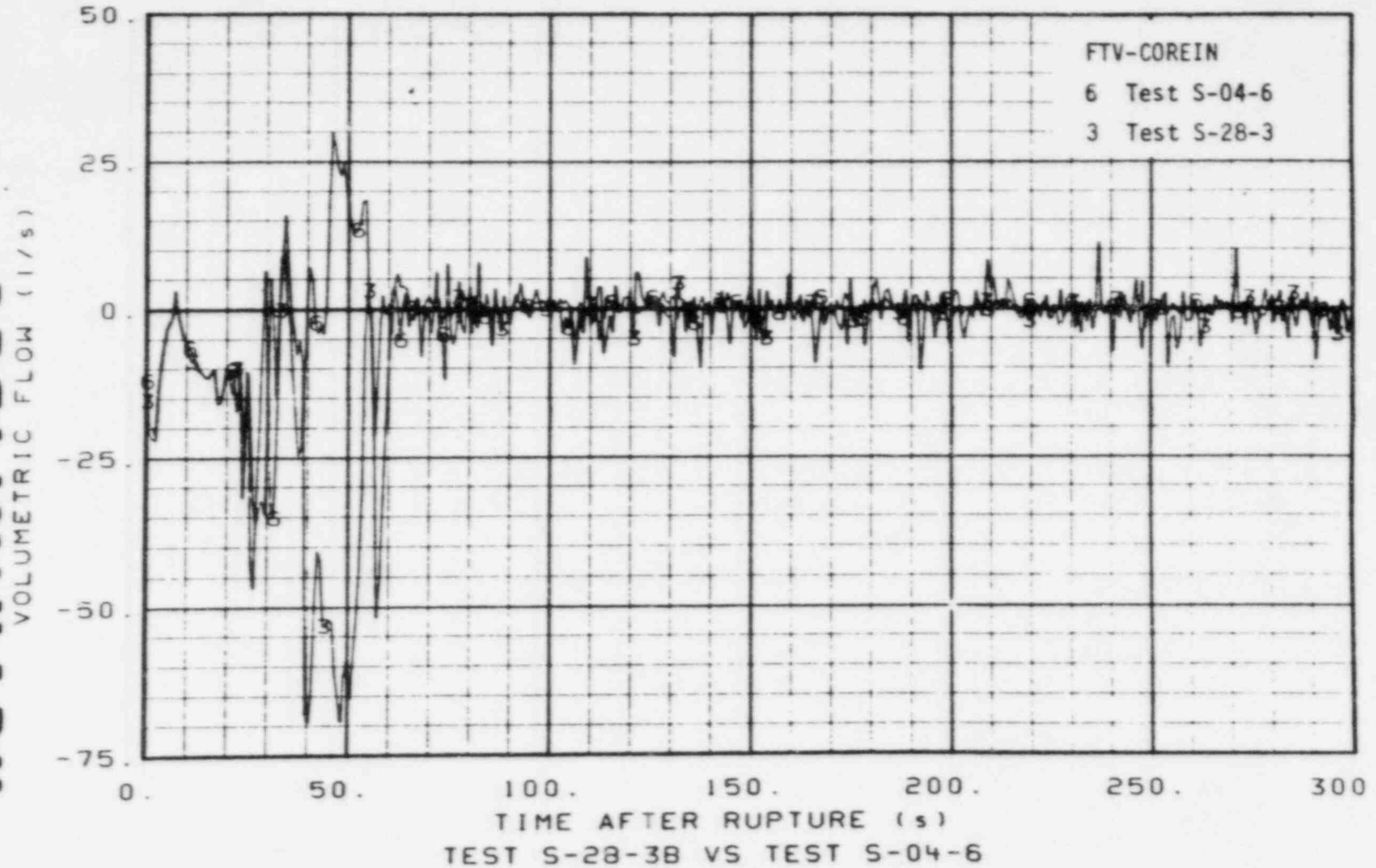

Figure 7. Comparison of Core Inlet Volumetric Flow - Tests S-28-3 and S-04-6

PRELIMINARY

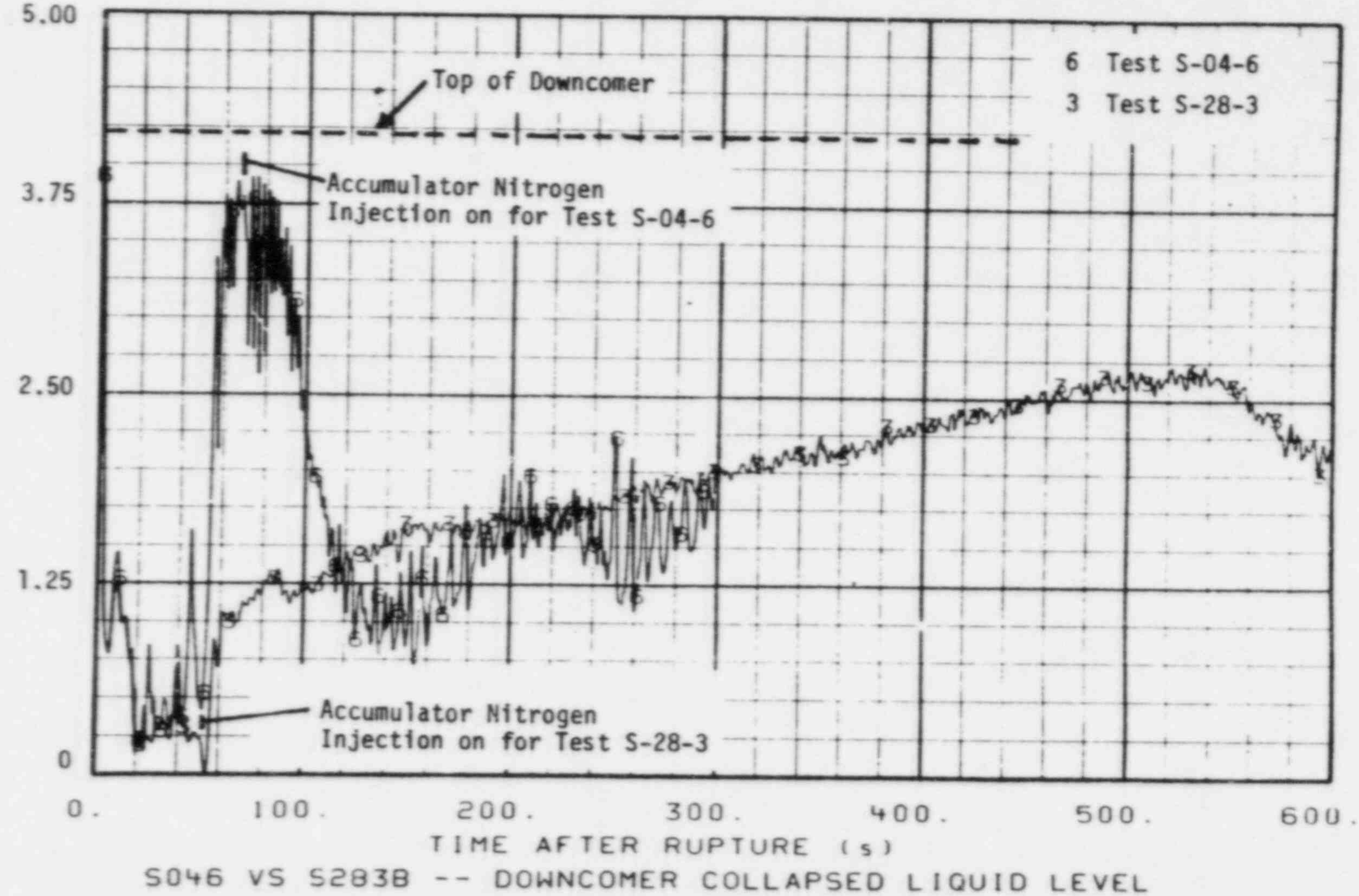

Figure 8. Comparison of Downcomer Collapsed Liquid Level - Tests S-28-3 and S-04-6

PRELIMINARY

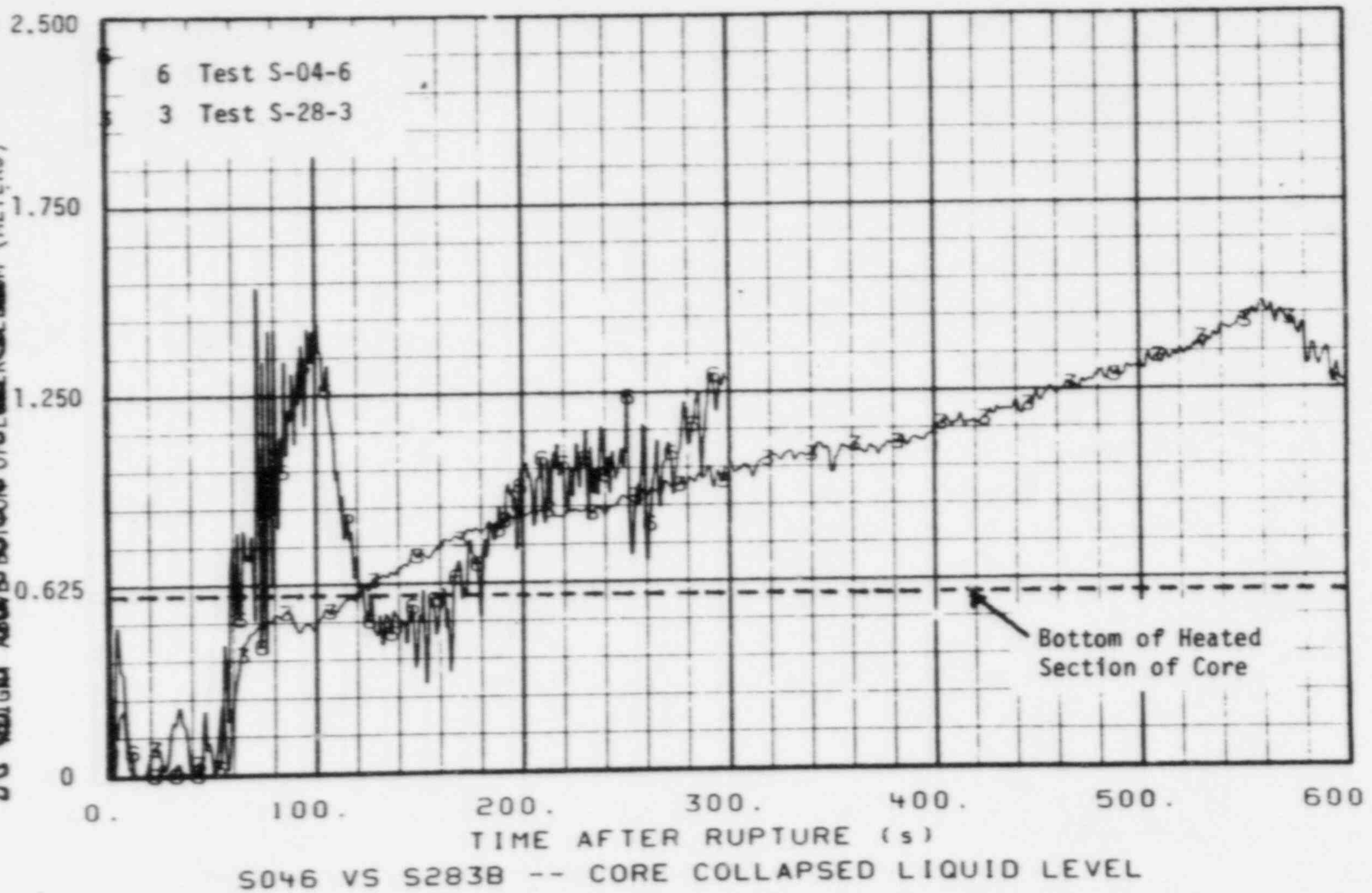

Figure 9. Comparison of Core Collapsed Liquid Level - Tests S-28-3 and S-04-6

PRELIMINARY

PRELIMINARY

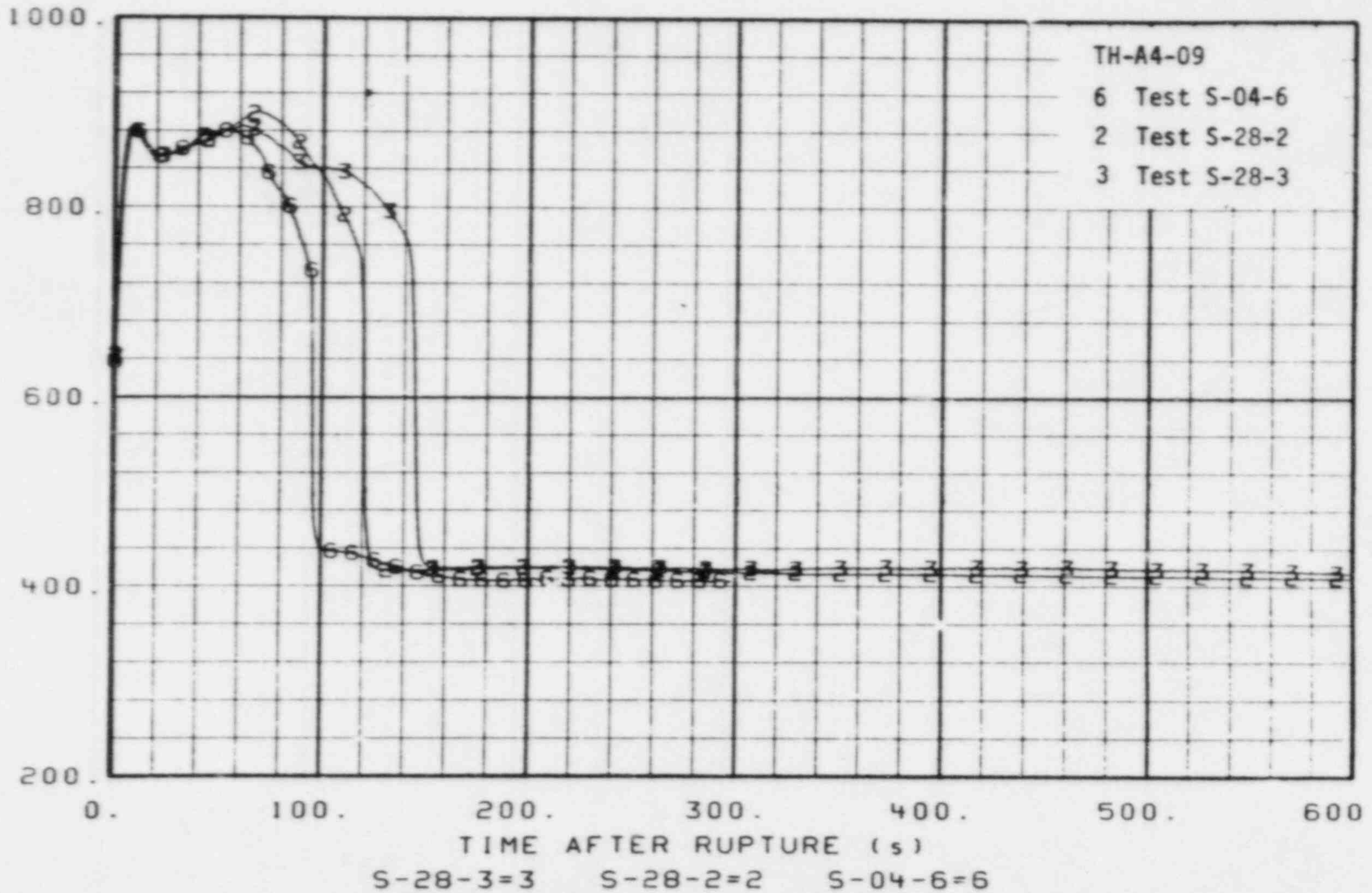

Figure 10. Comparison of Cladding Temperatures on Rod A4 at the 0.23 Meter Elevation - Tests S-28-2, S-28-3 and S-04-6

PRELIMINARY

PRELIMINARY

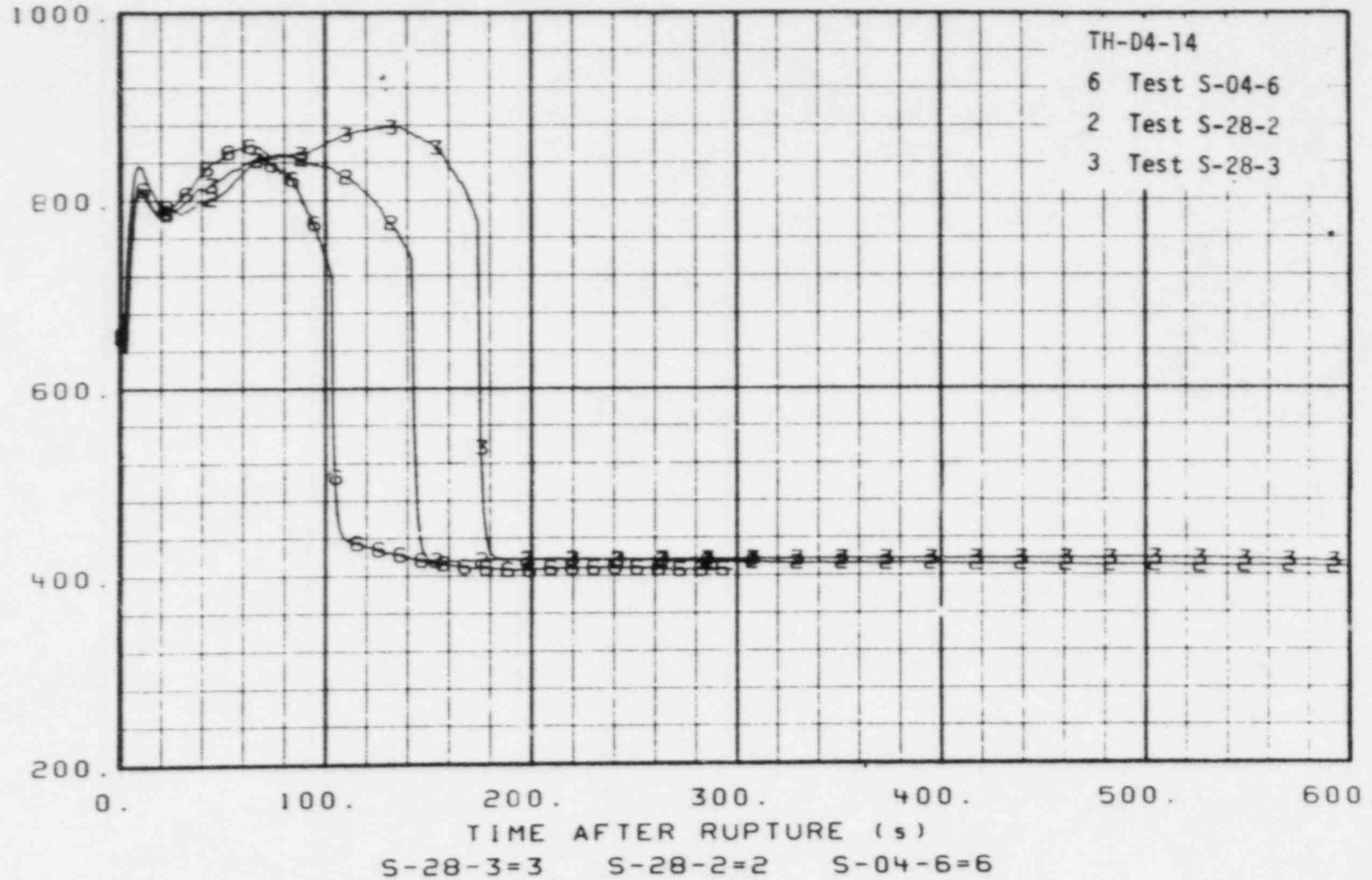

Figure 11. Comparison of Caldding Temperatures on Rod D4 at the 0.36 Meter Elevation - Tests S-28-2, S-28-3, and S-04-6

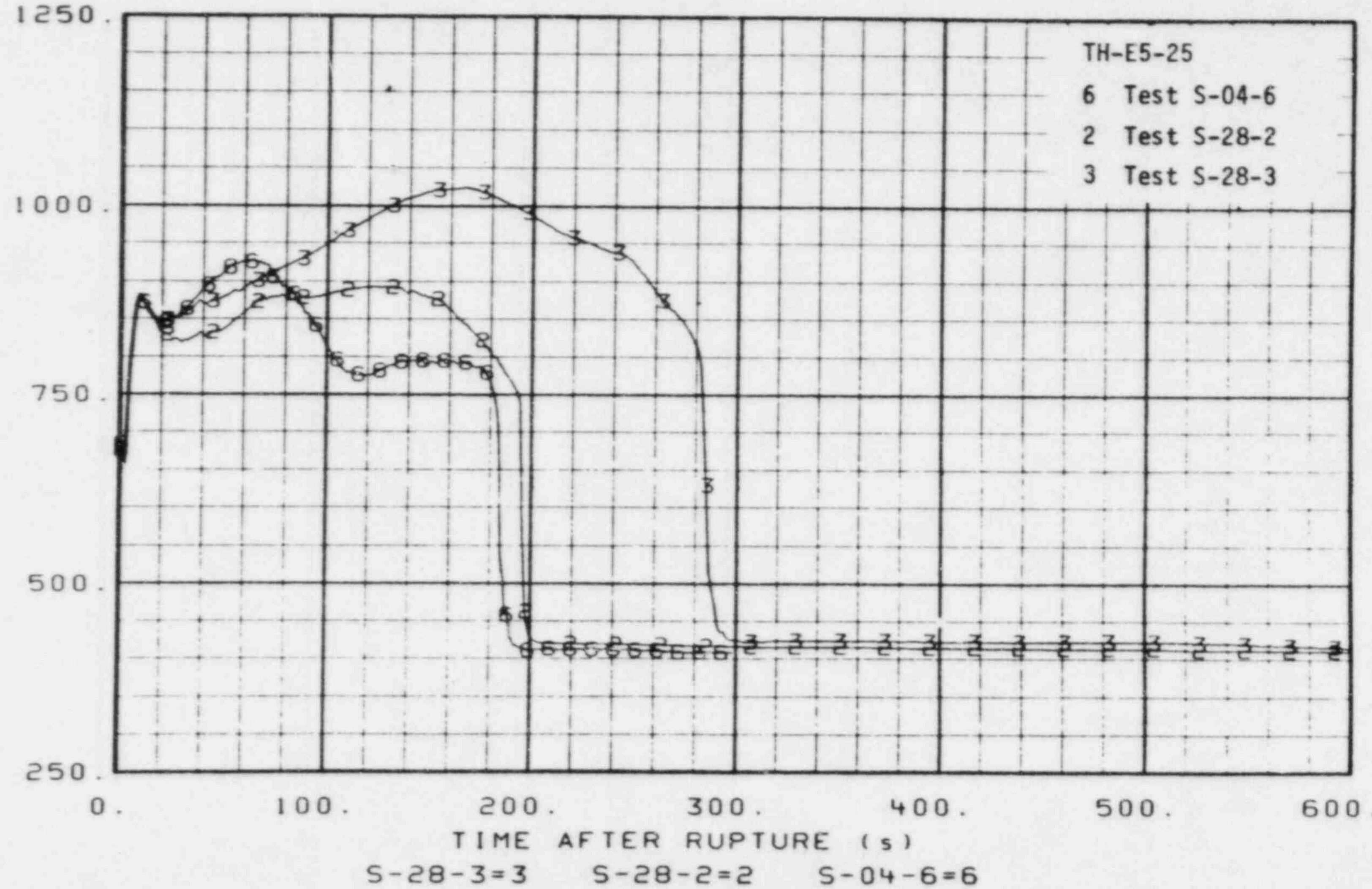

Figure 12. Comparison of Cladding Temperatures on Rod E5 at the 0.64 Meter Elevation - Tests S-28-2, S-28-3 and S-04-6

PRELIMINARY

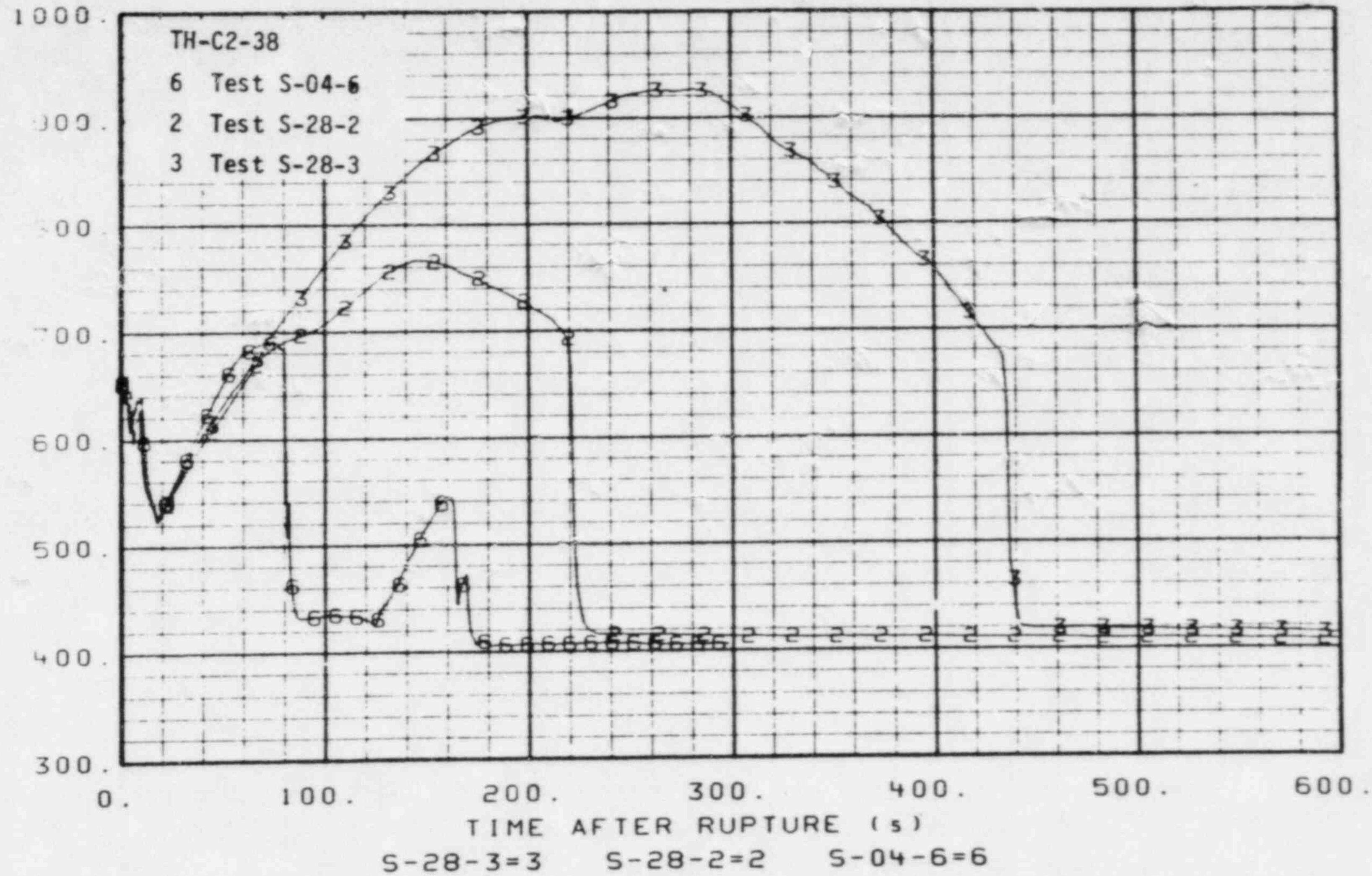

PRELIMINARY

PRELIMINARY

Figure 13. Comparison of Cladding Temperatures on Rod C2 at the 0.97 Meter Elevation - Tests S-28-2, S-28-3 and S-04-6

PRELIMINARY

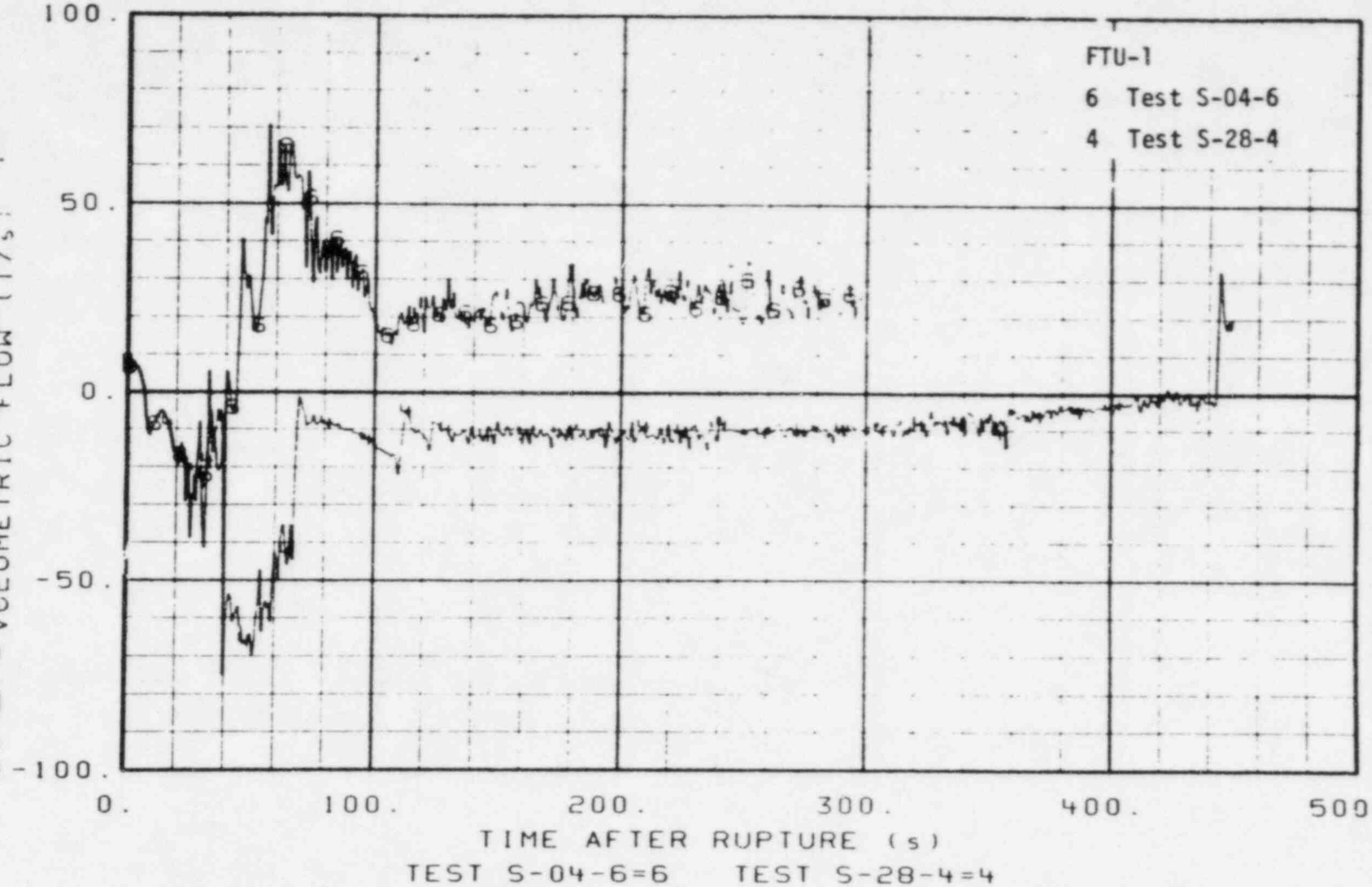

Figure 14. Comparison of Intact Loop Hot Leg Volumetric Flow Near the Vessel - Tests S-28-4 and S-04-6

PRELIMINARY

PRELIMINARY

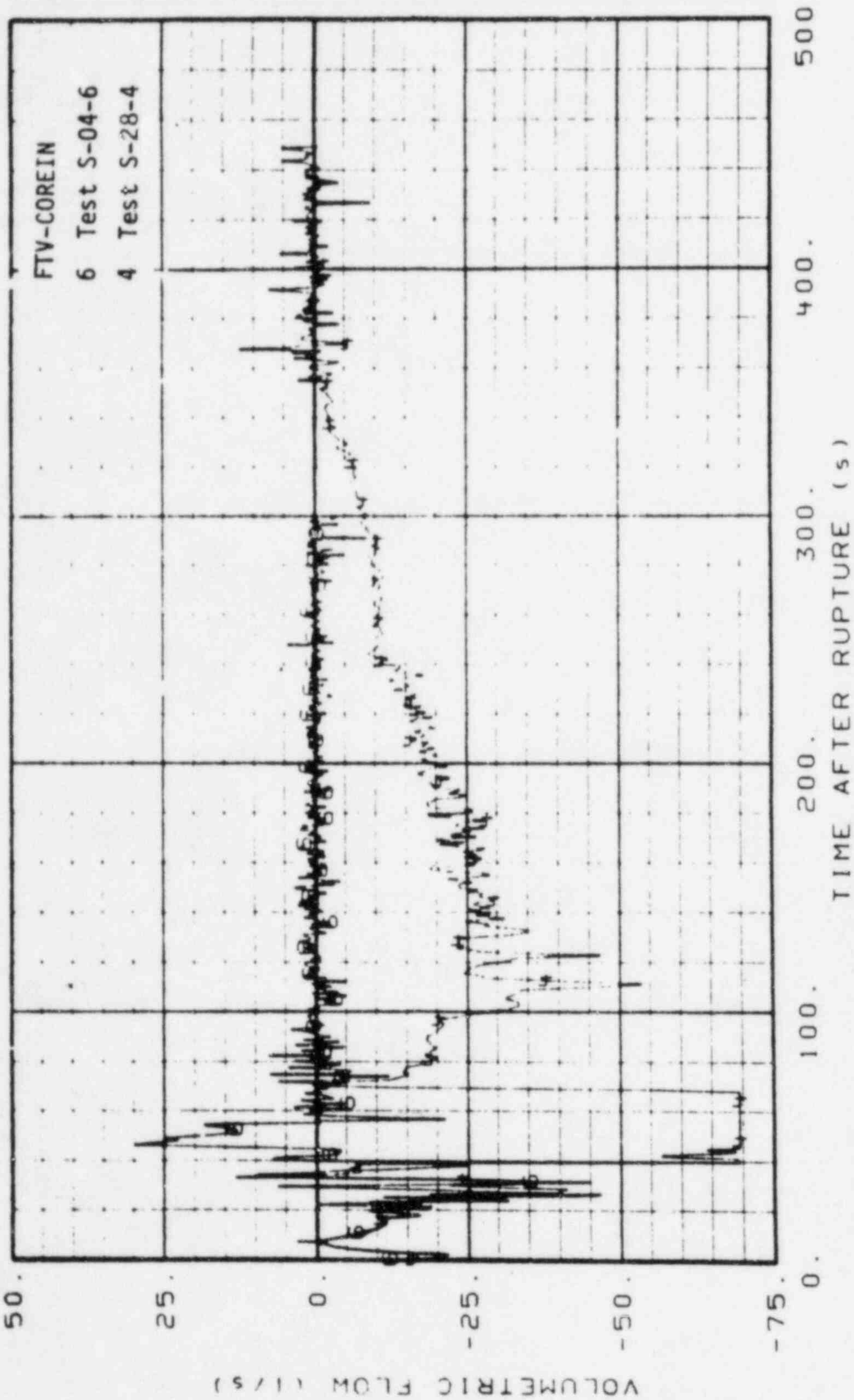

Figure 15. Comparison of Core Inlet Volumetric Flow - Tests S-28-4 and S-04-6

PRELIMINARY

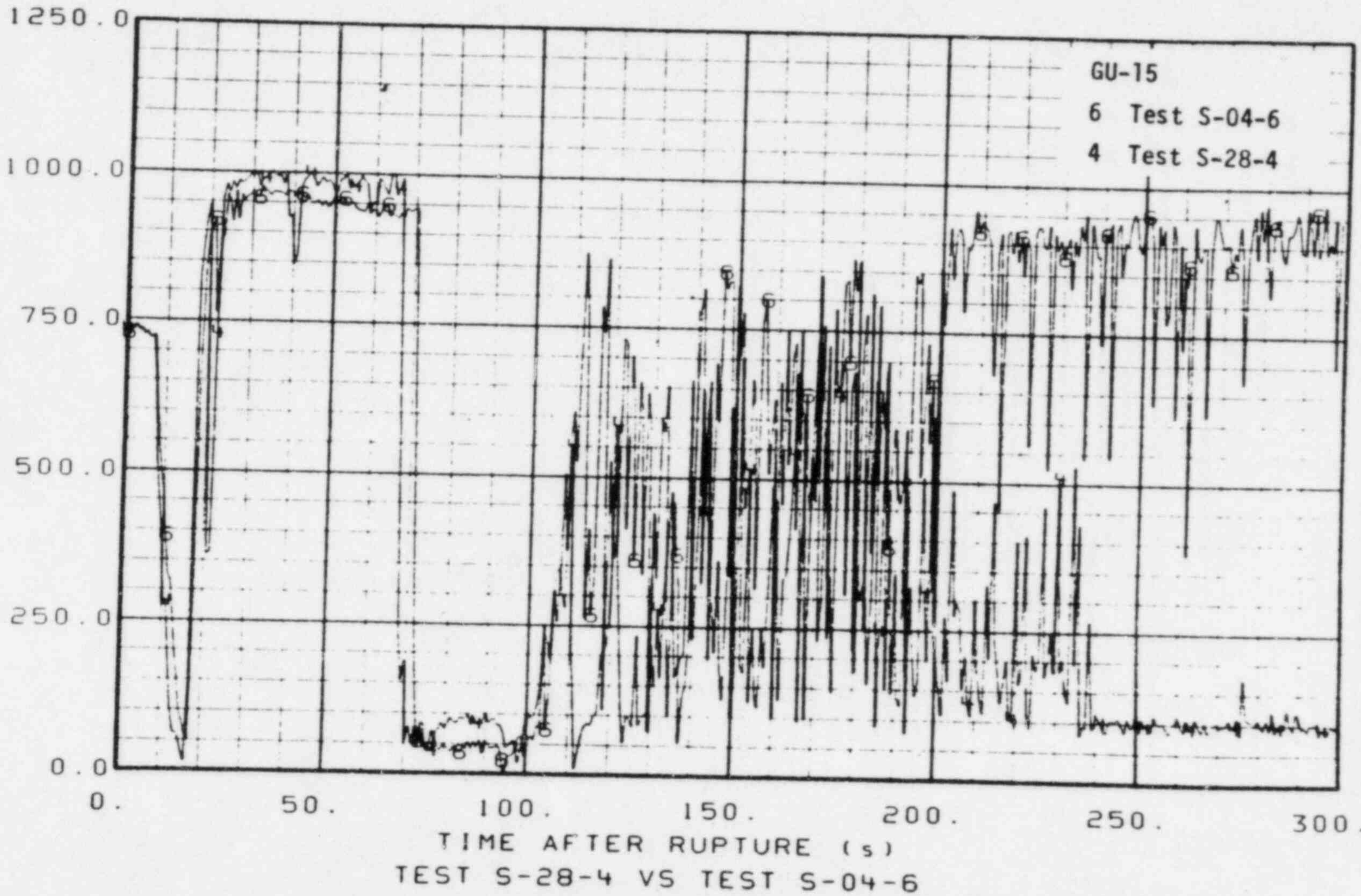

Figure 16. Comparison of Fluid Density in the Intact Loop Hot Leg Near the Vessel - Tests S-28-4 and S-04-6

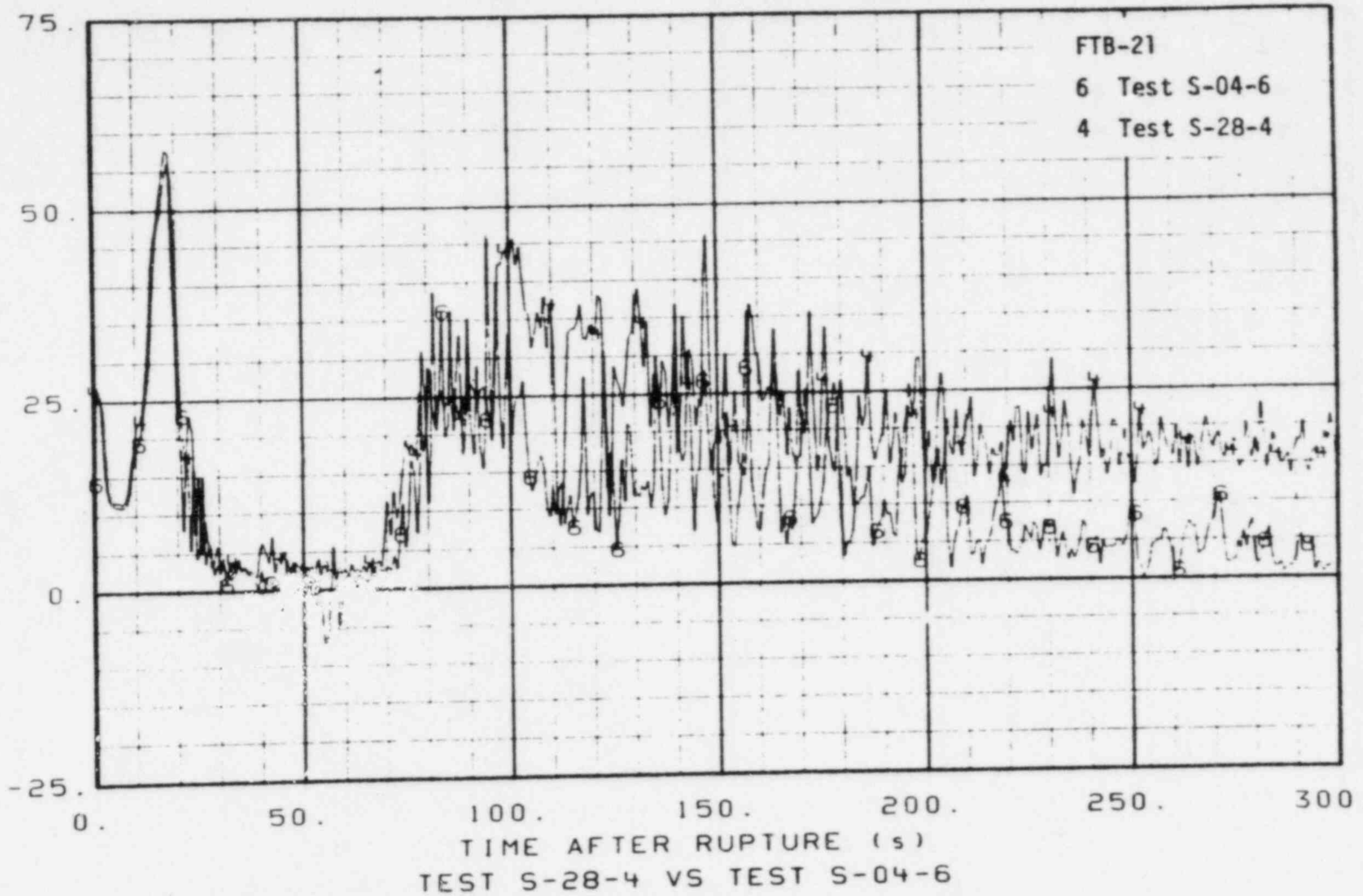

Figure 17. Comparison of Volumetric Flow in the Vessel Inlet Side of the Broken Loop - Tests S-28-4 and S-04-6

PRELIMINARY

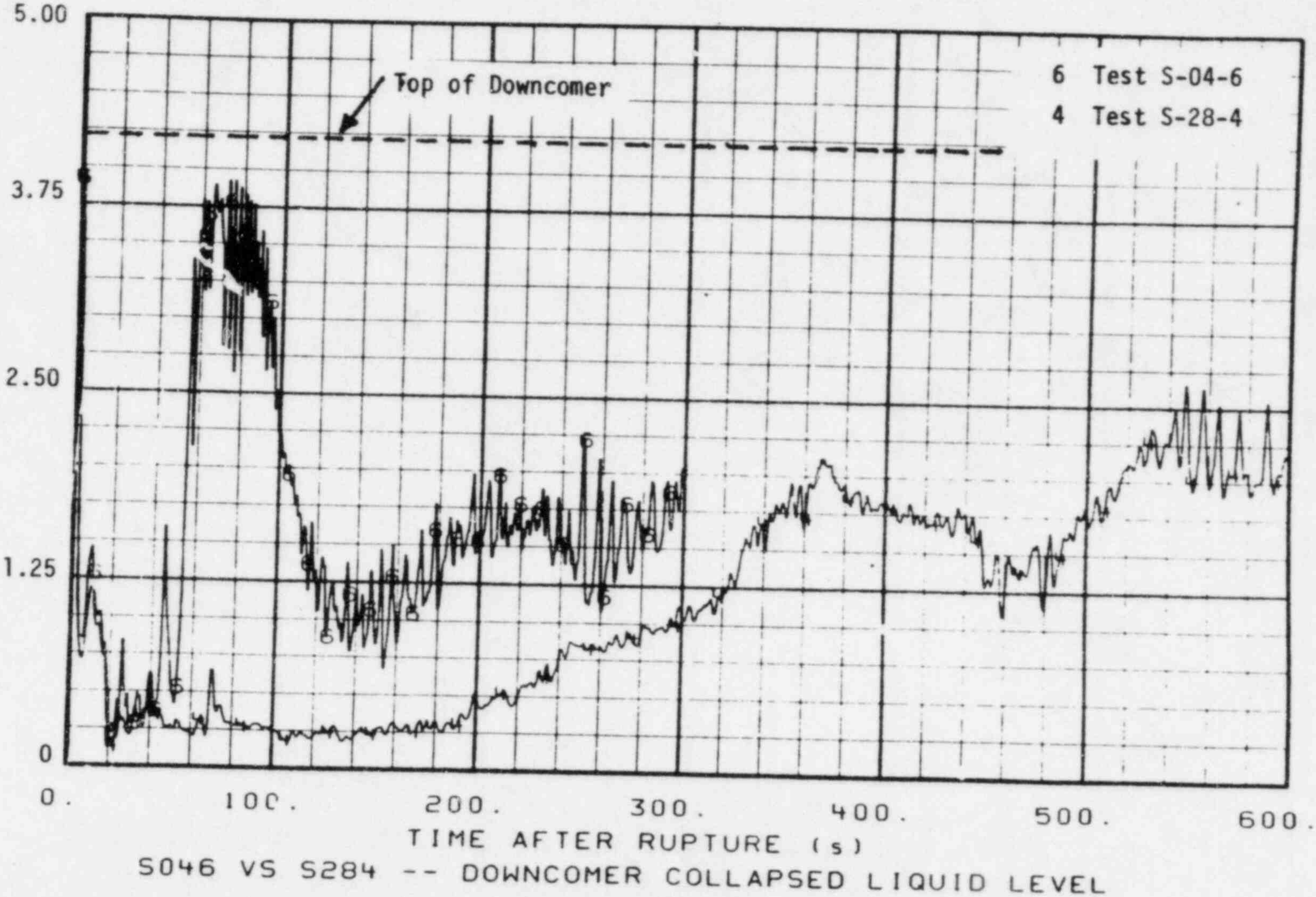

Figure 18. Comparison of Downcomer Collapsed Liquid Level - Tests S-28-4 and S-04-6

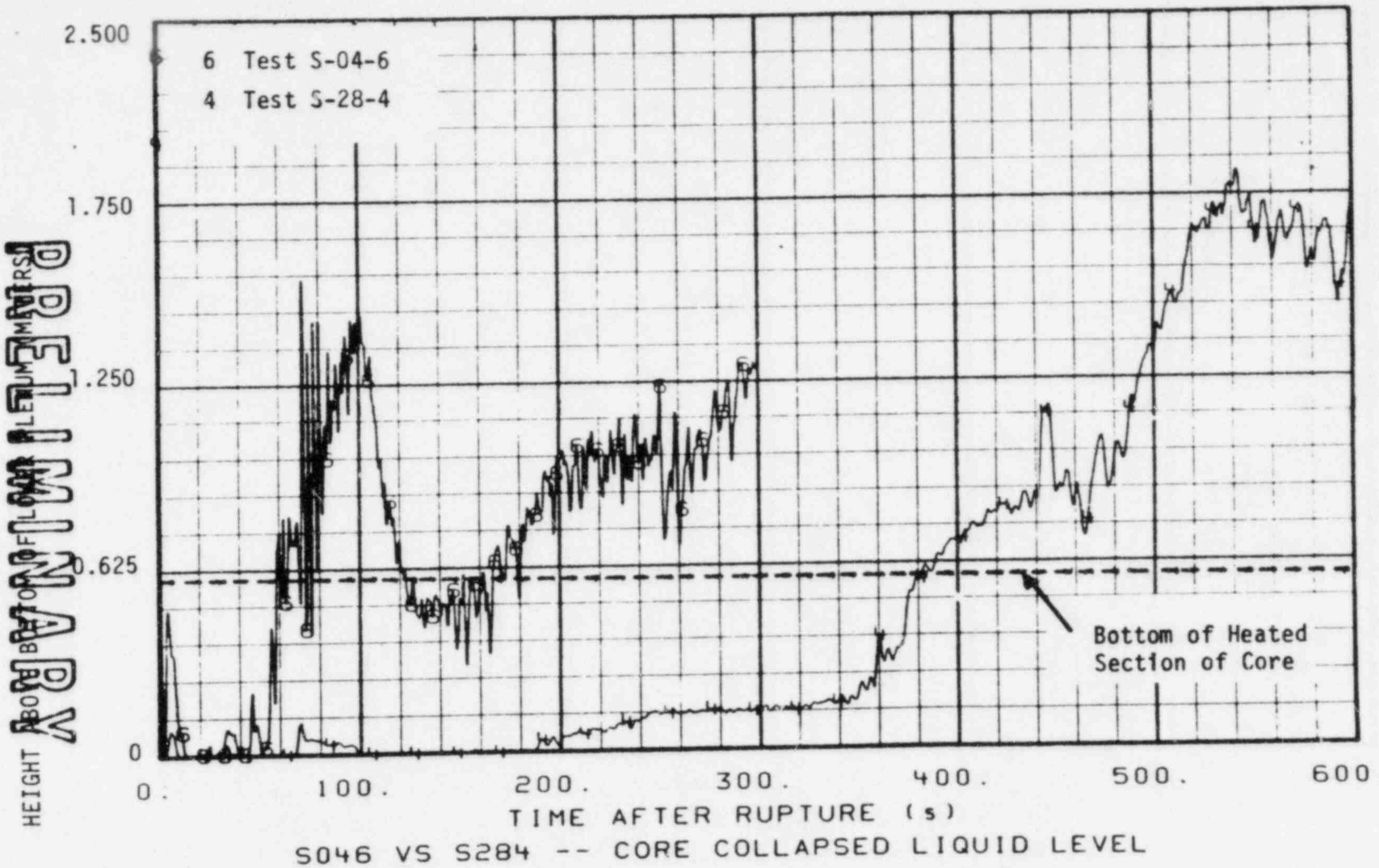

Figure 19. Comparison of Core Collapsed Liquid Level - Tests S-28-4 and S-04-6

PRELIMINARY

PRELIMINARY

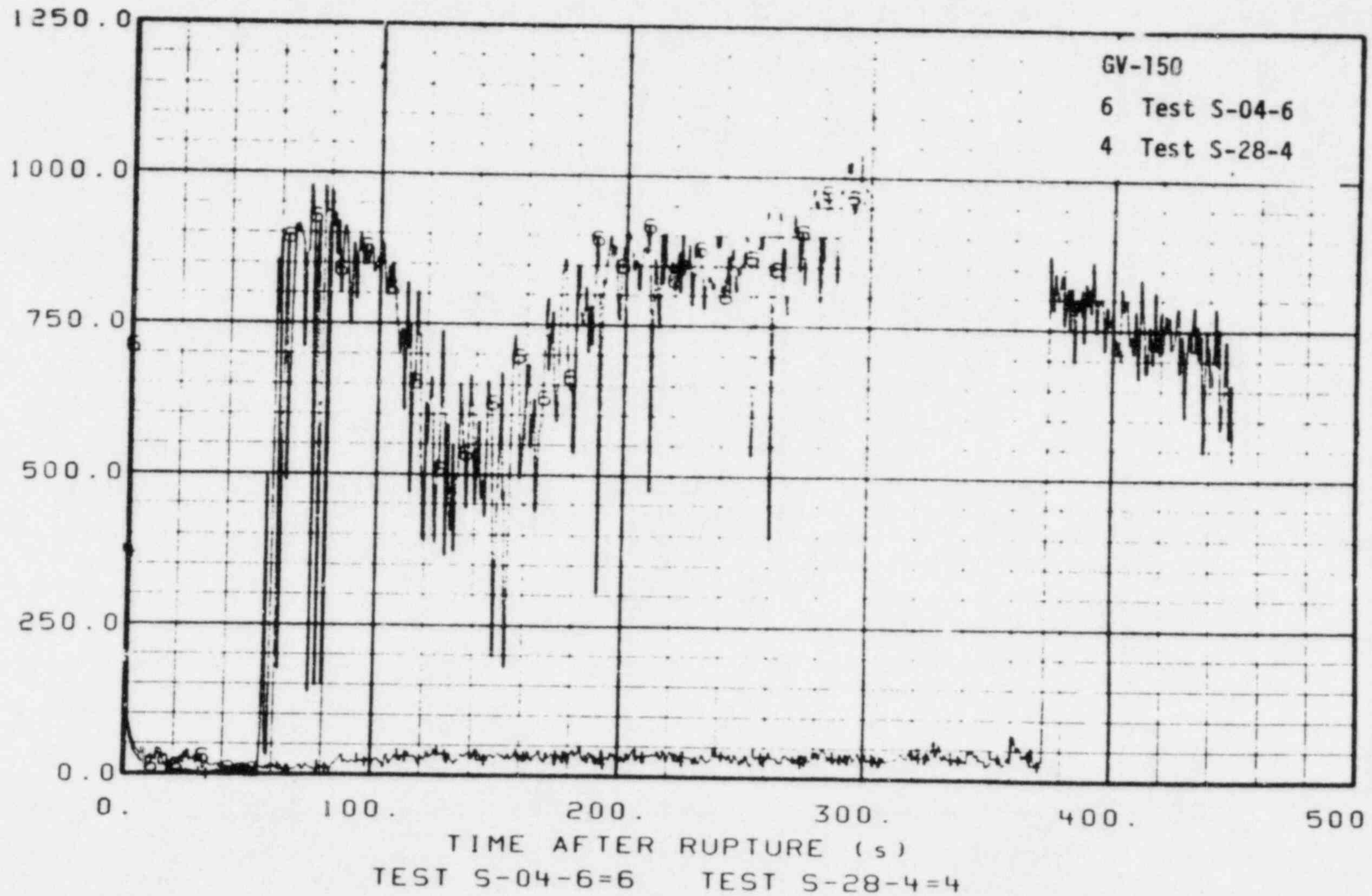

Figure 20. Comparison of Core Inlet Fluid Density - Tests S-28-4 and S-04-6

PRELIMINARY

PRELIMINARY

PRELIMINARY

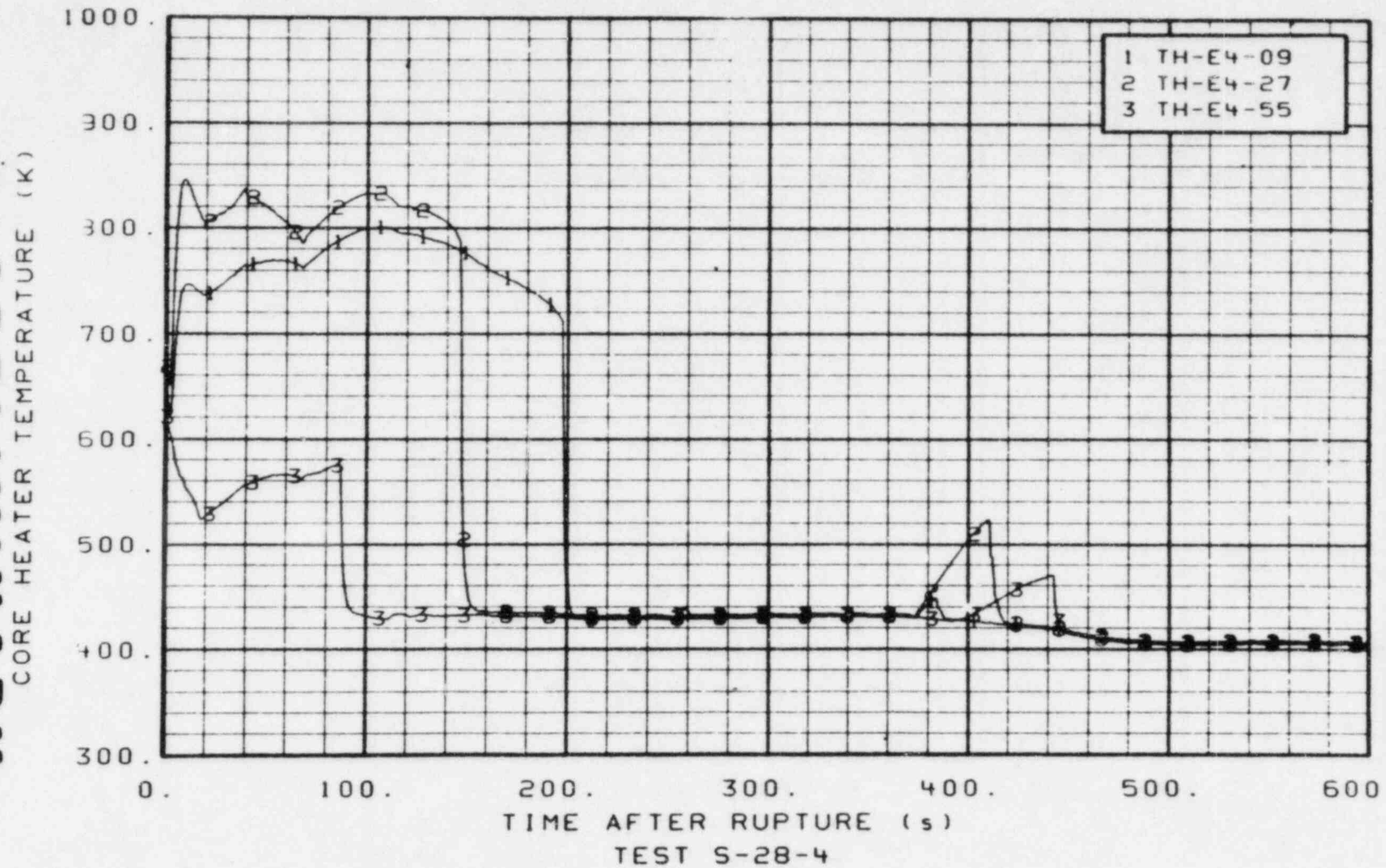

Figure 21. Cladding Temperatures on Rod E4 - Test S-28-4

PRELIMINARY

PRELIMINARY

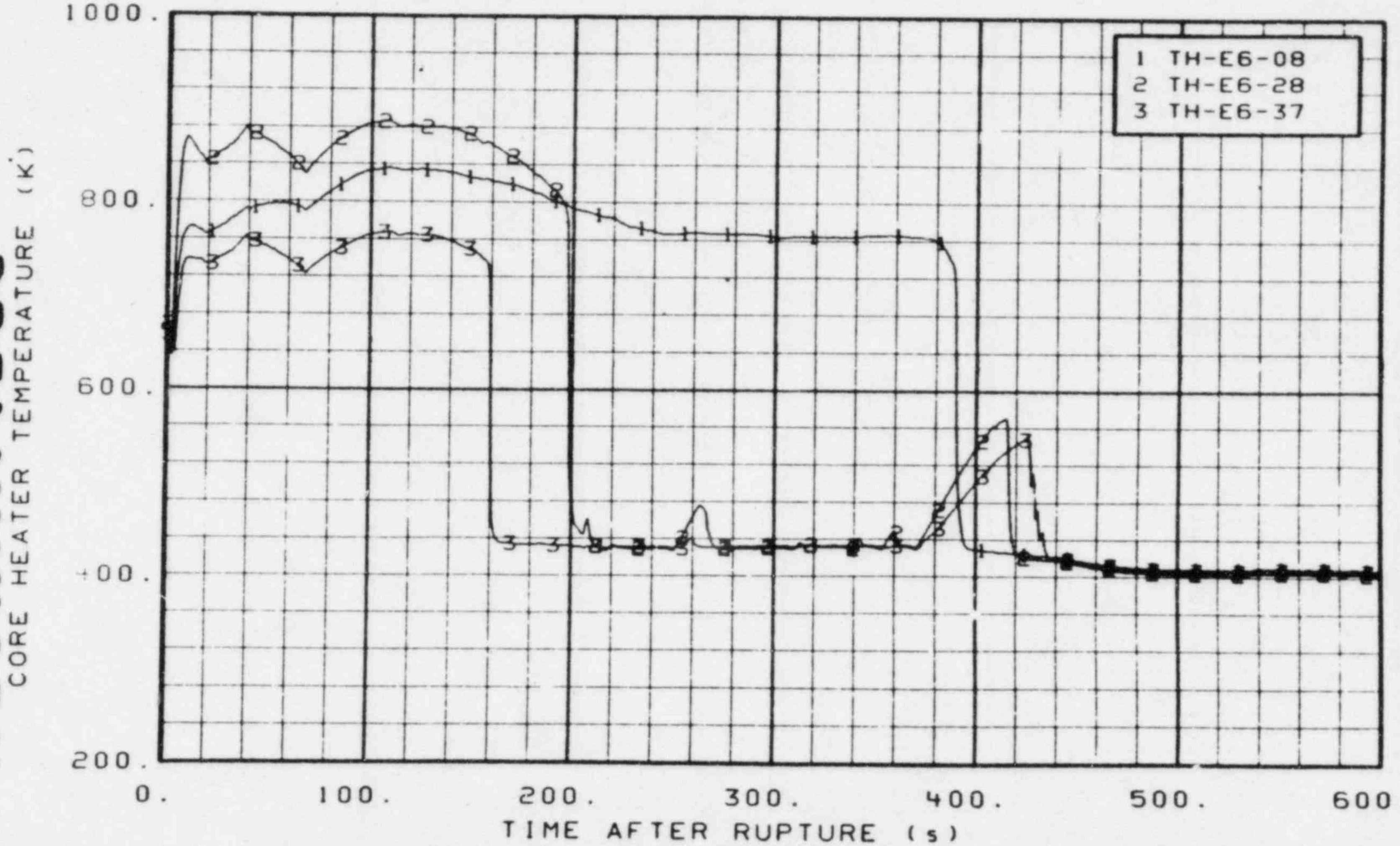

Figure 22. Cladding Temperatures on Rod E6 - Test S-28-4

PRELIMINARY

PRELIMINARY

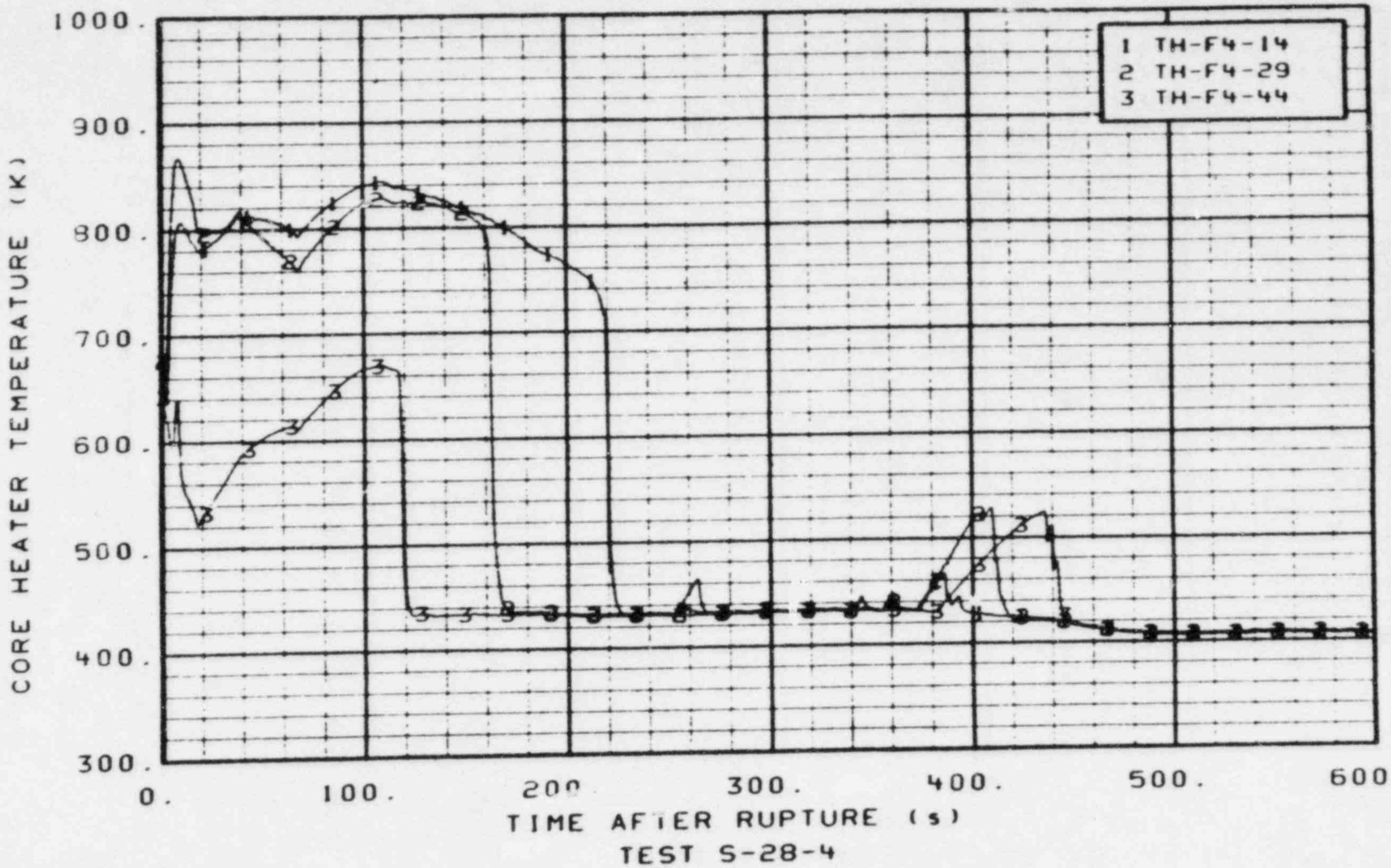

Figure 23. Cladding Temperatures on Rod F4 - Test S-28-4

PRELIMINARY

EG&G Idaho, Inc.

P. O. Box 1625
Idaho Falls, Idaho 83401

August 19, 1977

Mr. R. E. Tiller, Director
Reactor Operation and Program Division
Idaho Operations Office - ERDA
Idaho Falls, Idaho 83401

TRANSMITTAL OF QUICK LOOK REPORT FOR SEMISCALE MOD-1 STEAM GENERATOR TUBE RUPTURE TEST S-28-5 - DJO-179-77

Dear Mr. Tiller:

Attached is the Quick Look Report for Semiscale Mod-1 Test S-28-5 which was performed July 20, 1977. This integral blowdown-reflood test was conducted with a break configuration representative of a 200% double-ended offset shear cold leg break, and included the injection of a heated liquid from a pressurized accumulator tank to simulate a steam generator tube rupture flow initiated at the start of vessel refill. The primary objective of Test S-28-5 was to determine the effect on the system and core thermal-hydraulic response of a simulated steam generator tube rupture flow rate equivalent to the flow associated with the single-ended rupture of 20 tubes in a PWR steam generator. The secondary-to-primary flow rate for Test S-28-5 was near the center of an analytically determined range of tube rupture flow rates which could lead to high rod cladding temperatures.

During the period of steam generator tube rupture injection in Test S-28-5, the secondary-to-primary flow had a significant influence on the thermal-hydraulic response of the system and core. Because of the relatively large secondary-to-primary flow, reflood of the core was not initiated until about 290 seconds after rupture. As a result of the delay in the initiation of core reflood and the relatively poor cooling in the core during the period of downcomer and lower plenum refill, the peak cladding temperatures in Test S-28-5 were considerably higher than the temperatures obtained in the baseline test (Test S-04-6) or in the previous steam generator tube rupture tests with somewhat larger secondary-to-primary flow rates. The core maximum cladding temperature during reflood for Test S-28-5 was about 1208°K and occurred at the 0.66m elevation on rod F5 at about 315 seconds after rupture.

Very truly yours,

D. J. Olson, Manager
Semiscale Program

JMC:elp

Attachment

FOIA-84-884
C 10

cc: R. W. Barber, ERDA
R. S. Brodsky, ERDA
W. W. Bixby, NRC - 2
R. S. Boyd, NRC
S. Fabic, NRC
R. B. Foulds, NRC
R. F. Fraley, ACRS - 21
S. H. Hanauer, NRC
G. Kelly, NRC
S. Levine, NRC
W. C. Lyon, NRC
T. G. McCreless, ACRS
T. E. Murley, NRC
T. M. Novak, NRC
D. F. Ross, NRC
Z. R. Rosztoczy, NRC
R. M. Scroggins, NRC
B. Sheron, NRC
D. E. Solberg, NRC
V. Stello, NRC
R. L. Tedesco, NRC
L. S. Tong, NRC - 2
J. Block, CREARE
G. F. Brockett, ITI
D. M. Chapin, MPR
J. Cudlin, B&W
R. Denning, BCL
R. B. Duffey, EPRI
G. Fader, CE
G. Farber, IfR
P. Griffith, MIT
R. W. Kiehn, EG&G Idaho
W. Kirchner, LASL
M. Levenson, EPRI
W. Loewenstein, EPRI - 2
P. A. Lottes, ANL
J. V. Miller, W
H. P. Pearson, EG&G Idaho - 6
W. Riebold, JRCE
H. Seipel, DBF&T
D. G. Thomas, HNL
D. Trent, PNL
R. J. Beers, ERDA-ID